Accepted Manuscript

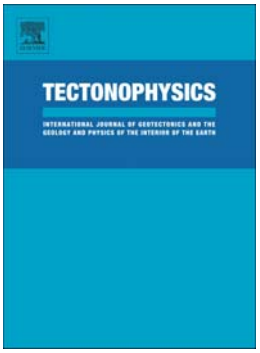

Orogen-perpendicular structures in the central Tasmanides and implications for the Paleozoic tectonic evolution of eastern Australia

Rashed Abdullah, Gideon Rosenbaum

PII: S0040-1951(16)30555-8
DOI: doi: 10.1016/j.tecto.2016.11.031
Reference: TECTO 127333

To appear in: *Tectonophysics*

Received date: 1 August 2016
Revised date: 17 November 2016
Accepted date: 20 November 2016

Please cite this article as: Abdullah, Rashed, Rosenbaum, Gideon, Orogen-perpendicular structures in the central Tasmanides and implications for the Paleozoic tectonic evolution of eastern Australia, *Tectonophysics* (2016), doi: 10.1016/j.tecto.2016.11.031

This is a PDF file of an unedited manuscript that has been accepted for publication. As a service to our customers we are providing this early version of the manuscript. The manuscript will undergo copyediting, typesetting, and review of the resulting proof before it is published in its final form. Please note that during the production process errors may be discovered which could affect the content, and all legal disclaimers that apply to the journal pertain.

ACCEPTED MANUSCRIPT

Orogen-perpendicular structures in the central Tasmanides and implications for the Paleozoic tectonic evolution of eastern Australia

Rashed Abdullah*, Gideon Rosenbaum

School of Earth Sciences, The University of Queensland, Brisbane 4072, Australia

*Corresponding author (Ph: +61470708404; Email: r.abdullah@uq.edu.au)

ABSTRACT

The curvilinear ~E-W structures of the southern Thomson Orogen are approximately orthogonal to the general ~N-S structural trend of the Tasmanides of eastern Australia. The origin of these orogen-perpendicular structures and their implications to tectonic reconstructions of eastern Gondwana are not fully understood. Here we use geophysical data to unravel the geometry, kinematics and possible timing of major structures along the boundary between the Thomson Orogen and the southern Tasmanides (Delamerian and Lachlan orogens). Aeromagnetic data from the southern Thomson Orogen show WNW, E-W and/or ENE trending structural grains, corresponding to relatively long wavelength linear geophysical anomalies. Kinematic analyses indicate strike-slip and transpressional deformation along these geophysically defined faults. Structural relationships indicate that faulting took place during the Benambran (Late Ordovician to Middle Silurian) and Tabberabberan (late Early to Middle Devonian) orogenies. However, some of the described crustal-scale structures may have developed in the Cambrian during the Delamerian Orogeny. Interpretation of deep seismic data shows that the crust of the southern Thomson Orogen is substantially thicker than the Lachlan Orogen crust, which is separated from the Thomson Orogen by the north dipping Olepoloko Fault. A major lithospheric-scale change across this boundary is also indicated by a contrast in seismic velocities. Together with evidence for the occurrence of Delamerian deformation in both the Koonenberry Belt and northeastern Thomson Orogen, and a significant contrast in the width of the northern Tasmanides versus the southern Tasmanides, it appears that the southern Thomson Orogen may represent the locus of orogen-perpendicular segmentation, which may have occurred in response to along-strike plate boundary variations.

ACCEPTED MANUSCRIPT

KEY WORDS: Gondwana, Tasmanides, Thomson Orogen, Olepoloko Fault, Delamerian Orogen.

1. INTRODUCTION

Orogenic belts commonly show evidence for large-scale orogen-perpendicular shear zones, but the origin of these structures is not always fully understood. Such structures may correspond to along-strike segmentation of fold-thrust-belts (Kley et al., 1999), or to plate boundary segmentation in response to trench retreat (Govers and Wortel, 2005; Rosenbaum et al., 2008). Alternatively, large orogen-perpendicular structures may correspond to earlier crustal structures that formed prior the development of the dominant orogenic structural grain. In any case, the recognition of large-scale orogen-perpendicular structures is indicative of a strongly heterogeneous crustal architecture that may have resulted from a complex history of deformation.

The Tasmanides in eastern Australia (Fig. 1a) is an assembly of Paleozoic to early Mesozoic orogenic belts, normally subdivided into the Delamerian, Lachlan, Thomson, Mossman and New England orogens (Glen, 2005). The structural grain of the Tasmanides is generally ~N-S, in accordance with the orientation of the paleo-Pacific plate boundary (Fergusson et al., 1986; Collins, 2002; Glen, 2005). In detail, however, the structure of the Tasmanides is more complex, involving a number of orogenic-scale curvatures (oroclines) (Rosenbaum et al., 2012; Musgrave, 2015) and orogen-perpendicular structures. The latter are particularly prominent along the boundary between the southern Thomson Orogen and the Lachlan and Delamerian orogens (Fig. 1a), where a curvilinear ~E-W structural trend contrasts the dominant ~N-S tectonic grains of the Tasmanides (Fig. 1b, c). The origin of these (~E-W) structural features is controversial (Burton, 2010; Glen et al., 2013; Klootwijk, 2013; Burton and Trigg, 2014; Glen et al., 2014), partly because of the very limited exposure of the Thomson Orogen in central Queensland and northwestern New South Wales (Fig. 1a). The vast sedimentary cover of the Thomson Orogen means that our understanding of this orogen is mainly derived from geophysical interpretation and sparse drill holes (Finlayson and Leven, 1987; Finlayson et al., 1988; Finlayson et al., 1990; Finlayson, 1993; Spampinato et al., 2015a; Spampinato et al., 2015b; Purdy et al., 2016) (Fig. 1b, c). Nevertheless, this part of the Tasmanides may provide fundamental information on the Paleozoic tectonic evolution of eastern Australia. In particular, key questions on the crustal architecture of the Tasmanides

ACCEPTED MANUSCRIPT

could be resolved if we understand the origin of the ~E-W structures in the southern Thomson Orogen.

The aim of the paper is to unravel the 3D geometry of crustal scale structures along the boundary between the southern Thomson, Delamerian and Lachlan orogens, and to understand the possible tectonic implications of these structures. We use a combination of 2D seismic reflection profiles, aeromagnetic data, and gravity data to determine the structural trends, geometry and kinematics of major fault systems along the Thomson-Delamerian-Lachlan boundary. These crustal-scale structures are then discussed in the context of the geodynamic evolution of the Tasmanides.

2. GEOLOGICAL SETTING

The Tasmanides of eastern Australia (Fig. 1a) represent a prolonged history of subduction along the Gondwanan margin from the Cambrian to Triassic (Foster and Gray, 2000; Veevers, 2004; Glen, 2005; Glen et al., 2013). The timing of orogenesis generally becomes younger from west to east. The orogenic assembly has been described as an accretionary orogen (Cawood et al., 2011) that has been subjected to alternating periods of trench retreat and advance (Collins, 2002). The most pronounced orogenic cycles are known as the Delamerian Orogeny (~515-490 Ma) (Foden et al., 2006), Benambran Orogeny (~460-425 Ma), Tabberabberan Orogeny (~390-380 Ma), Kanimblan Orogeny (~360-340 Ma) (Cas, 1983; Coney et al., 1990; Glen, 1992; Gray and Foster, 1997; Thalhammer et al., 1998; Veevers, 2000; Glen, 2005) and Hunter-Bowen Orogeny (~260-230 Ma) (Fergusson, 1991; Holcombe et al., 1997).

The Delamerian Orogen is exposed along the state border between South Australia and Victoria (Fig. 1a) and farther north in the Koonenberry Belt (southwestern New South Wales). The latter constitutes the western section of the ~E-W gravity anomalies along the boundary with the southern Thomson Orogen (Figs. 1 and 2). The three distinct NNW-trending structural domains of the Koonenberry Belt are: a) Bancannia Trough to the west; b) Wonnaminta Zone in the middle; and, c) Kayrunnera Zone to the east (Fig. 2a). Ediacaran to Early Ordovician successions of the Koonenberry Belt represent an early episode of deposition on a continental passive margin and a later phase of arc volcanism (Mount Wright Volcanic Arc) (Greenfield et al., 2010; Greenfield et al., 2011; Johnson et al., 2016). The Ediacaran to Middle Cambrian rocks were deformed in response to contractional events

ACCEPTED MANUSCRIPT

associated with the Delamerian Orogeny (Greenfield et al., 2010). In the northeastern part of the Koonenberry Belt, Cambro-Ordovician packages occur above a post-Delamerian angular unconformity (Webby, 1978). These rocks record younger phases of deformation associated with the Benambran, Tabberabberan and Kanimblan orogenies (Neef, 2004; Greenfield et al., 2010). Another province within the region is the Warburton Basin, which is located northwest of the Koonenberry Belt (Fig. 1a). This basin is interpreted to be a Cambrian-Ordovician back-arc basin (Radke, 2009). The Warburton Basin is covered by Late Carboniferous to Mesozoic sedimentary rocks of the Cooper, Pedrika and Eromanga basins (Purdy et al., 2013).

Cambrian to Carboniferous rocks in the Lachlan Orogen (Fig. 1a) record Benambran, Tabberabberan and Kanimblan deformation (Coney et al., 1990; Glen, 1992; Veevers, 2000; Glen, 2005). In the northern Lachlan Orogen, the major stratigraphic successions include: 1) Lower-Middle Ordovician metamorphosed turbidites of the Girilambone Group (Burton, 2010; Burton et al., 2012); 2) Lower Devonian rocks of the Cobar Supergroup (Glen et al., 1996); and 3) late Lower Devonian to Upper Devonian rocks of the Mulga Downs Group (Carty and Moffitt, 2001; Hegarty, 2011) (Figs. 2c and 3). Silurian to Devonian I- and S-type granitoids are intruded into the metasedimentary successions of the Lachlan Orogen (Figs. 2c and 3) (Black, 2006; Blevin, 2011; Hegarty, 2011; Fraser et al., 2014). In the east-central Lachlan Orogen, the ~N-S trending Ordovician to Early Silurian Macquarie Arc is a key component (Fig. 1b, c), comprising of mafic to intermediate volcanic rocks, volcaniclastic rocks, and interbedded limestone and chert (Glen et al., 2002; Fergusson, 2009).

The Thomson Orogen (Fig. 1a) comprises of Cambrian-Ordovician metasedimentary and Silurian to Devonian igneous rocks (Figs. 2c and 3). Limited rock exposures that are thought to be parts of the basement of the Thomson Orogen occur along the northeastern edge of the orogen (Anakie, Charters Towers, Greenvale and Barnard provinces; Fig. 1a) (Fergusson et al., 2013; Purdy et al., 2013; Purdy et al., 2016). Neoproterozoic metasedimentary rocks of these provinces record Cambrian (~510-500 Ma) deformation and greenschist-amphibolite facies metamorphism (Withnall et al., 1995; Withnall et al., 1996; Fergusson et al., 2001; Nishiya et al., 2003; Fergusson et al., 2013; Verdel et al., 2016). Evidence of younger contractional deformation has also been recognized in the Anakie Inlier and interpreted to be associated with the Benambran Orogeny (Fergusson et al., 2013).

ACCEPTED MANUSCRIPT

A prominent geophysical feature south of the Anakie Inlier is the Nebine Ridge, which is defined by a broad gravity and subsurface basement high (Fig. 2a) (Purdy et al., 2013). Basement cores from Nebine Ridge show multiply deformed metamorphic rocks ranging from lower-greenschist to amphibolite facies, similar to the rocks found in the Anakie-Charters Towers provinces (Murray, 1994; Withnall et al., 1995). Maximum constraints on the depositional age of metasedimentary rocks from the Nebine Ridge are 520±10 Ma (Kositcin et al., 2015).

The Anakie-Charters Towers-Greenvale provinces (and possibly the Nebine Ridge in the subsurface) record deformation equivalent to the Delamerian Orogeny in the Koonenberry Belt. This raises a question on the spatial link between the Koonenberry Belt (i.e., the Delamerian Orogen) and the outcrops of the Thomson Orogen farther to the northeast. The possible link between these regions is the southern Thomson Orogen, which was interpreted by Glen et al. (2013) as comprising a Neoproterozoic basement. The interpretation was based on a relatively small number of Neoproterozoic (~577 Ma) U-Pb zircon ages from the Warraweena Volcanics. However, whether or not these ages represent the timing of magmatism is a matter of debate [see Burton and Trigg (2014)].

The nature of the Thomson-Lachlan boundary is also controversial (Burton and Trigg, 2014; Glen et al., 2014). Some authors suggested that the boundary is represented by the Olepoloko Fault and Louth-Eumarra Shear Zone (Figs. 1c and 2b) (Murray and Kirkegaard, 1978; Stevens, 1991; Glen et al., 1996; Glen, 2005; Glen et al., 2013). The distinction was made based on the ~E-W structural discordance at the southern Thomson Orogen recognized in gravity and aeromagnetic data (Figs. 1b, c and 2a, b). In contrast, Burton and Trigg (2014) and Burton (2010) have argued that these ~E-W structures reside exclusively within the Lachlan Orogen and do not represent the actual boundary between the Thomson and Lachlan orogens. Dunstan et al. (2016) have recently shown that a substantial component of dextral kinematics has been accommodated along the Louth-Eumarra Shear Zone and related structures. Nonetheless, the kinematics of many other crustal-scale structures remains unresolved.

3. METHODS

Potential field (gravity and magnetic) data can provide insights into crustal architecture and terrane analyses, and are specifically vital for investigating regions of limited rock exposures

ACCEPTED MANUSCRIPT

(Whiting, 1986; Jessell and Valenta, 1996; Gunn et al., 1997; McLean and Betts, 2003; McLean et al., 2008; Stewart and Betts, 2010). Although interpretation of gravity and aeromagnetic data does not necessarily provide unique solutions (Betts et al., 2003; McLean and Betts, 2003; McLean et al., 2008; Stewart and Betts, 2010), the combined use of geological and geophysical constraints, such as borehole and seismic data, may significantly reduce the ambiguity, and serve as a powerful tool for investigating inaccessible terranes.

In order to identify and interpret major lineaments, we used gridded aeromagnetic data with spatial resolution of 50, 80, 250 and 400 m, and gravity data with spatial resolution of 500, 800 and 1000 m, provided by the Geological Survey of Queensland, Geological Survey of New South Wales and Geological Survey of South Australia. A number of data processing and image processing algorithms (Table 1) were applied to gravity and magnetic data (using Geosoft's Oasis Montaj^{TM} software) in order to enhance or remove wavelengths in the datasets and highlight different crustal levels. The gridded potential field datasets allowed us to recognize geophysically defined faults. Fault kinematics was interpreted based on offset and dragging of anomalous features.

Table 1. Nomenclature, definition and use of selected methods of processing and imaging Bouguer gravity and aeromagnetic data

	Description	Application
Data processing		
Reduced-to-pole (RTP)	An algorithm that applied on TMI gridded data to remove the effects of magnetic inclination and declination of the main field on the anomaly shapes.	Locating anomalies directly above their possible sources to show the true geometry of the magnetic bodies (Swain, 2000; Cooper and Cowan, 2005).
Tilt derivative	The arc tangent of the ratio of first vertical derivative and the total horizontal derivative, irrespective of the amplitude or wavelength of the geophysical anomalies.	Improving vertical contacts between the source bodies (geological edges and fault lineaments for both deep and shallow features) and geophysical responses of weak anomalies (Miller and Singh, 1994).
Upward continuation	Bringing the plane of measurement farther from the source.	Suppressing the shallower features and highlighting deep structural features (Gibert and Galdeano, 1985).
Image processing		

ACCEPTED MANUSCRIPT

Colour-shaded image	Overlaying a colour table of the data with shaded greyscale image of the same dataset.	Providing colour and textural ranges that allow the differentiation between geophysical domains (Stewart and Betts, 2010).
Composite image	Layering of two different datasets or differently processed images.	Enabling correlation of spatially coincident features within the datasets (Stewart and Betts, 2010).

Three regional deep seismic transects (99AGS C1, 05GATL 1 and 05GATL 2) and one shallow seismic transect (DMR 98-02) were used to complement the structural interpretation of the potential field data and to define crustal architectures. These seismic data were obtained from Geoscience Australia and Geological Survey of New South Wales. The seismic sections are migrated and displayed assuming an average crustal velocity of 6 km s-1, which provided a vertical to horizontal scale of approximately 1:1. Seismic impedance and reflection geometry allow us to recognize the mantle (almost reflection free), crust (reflective lower crust and weakly reflective upper crusts) and sedimentary packages (parallel to sub-parallel reflectors with fair continuity). Faults can be interpreted based on the offset of a prominent reflector (or a reflection package), and onlapping reflection configurations allow the recognition of syn-kinematic packages.

4. RESULTS

4.1. Koonenberry Belt

4.1.1. Bancannia Trough

The Bancannia Trough is the westernmost part of the Koonenberry Belt. It is characterized by a broad gravity low (Figs. 2a and 4a) that likely reflects a thick succession of sedimentary or metasedimentary rocks within the trough. Large prominent magnetic anomalies parallel to the axis of the trough (Figs. 2b and 4b) may correspond to rocks with high magnetic susceptibilities (e.g., volcanic rocks) that possibly occur below the sedimentary successions.

The seismic transect (99AGS C1, Fig. 4c, d) shows that the Bancannia Trough is separated from Precambrian rocks (Curnamona Craton; Fig. 1a) by a steeply northeast-dipping normal fault that extends down to ~0.5-7.0 seconds TWT (Fig. 4d). At an approximate depth of 30-40 km (10-13 seconds TWT, Fig. 4), this fault merges with a major gently northeast-dipping

ACCEPTED MANUSCRIPT

structure, named Bancannia Shear Zone. In the eastern part of the Bancannia Trough, a steeply southwest-dipping fault is recognized.

Interpretation of the seismic transect (Fig. 4d) across the Bancannia Trough shows a very weak shallowly southwest-dipping reflection package at ~40-45 km depth (~13-15 seconds TWT), which corresponds to the Moho. Above the Moho, the crust is characterized by non-reflective to weakly reflective packages (at ~3-12 seconds TWT). However, few reflectors (at ~2.5-5.0 seconds TWT) show relatively strong amplitude that is possibly associated with the presence of volcanic rocks (Fig. 4d). This package of rocks is the possible correlative of the Cambrian Mount Wright Volcanics (Greenfield et al., 2011). Above the volcanic rocks (at ~5-10 km depth or ~1.5-3 seconds TWT), a package of gently dipping, parallel to semi-parallel reflectors, are bounded by two unconformities above and below (Fig. 4d). These refection packages possibly correspond to Late Cambrian to Early Ordovician successions (Mills and David, 2004). Above the unconformity (~1-2 seconds TWT), gentle onlapping reflectors to the southwest show a wedge-shaped half-graben structure (Fig. 4d). This wedge-shaped syn-rift package corresponds to Early to Middle Devonian sedimentary rocks (Mills and David, 2004). Reflectors are gently onlapping northeast to an unconformity surface at the top of this syn-rift unit. These reflectors possibly represent Middle to Late Devonian rocks (Mills and David, 2004). The onlapping reflection geometry and minor folding of all three packages indicate that the half graben was subjected to basin inversion during or after the deposition of the Middle to Late Devonian rocks (Fig. 4d).

4.1.2. Wonnaminta Zone

The NNW-trending Lawrence Fault defines the boundary between the Bancannia Trough and the Wonnaminta Zone (Fig. 2a, b). The aeromagnetic signature of the Wonnaminta Zone is characterized by intense, short-wavelength, linear or curvilinear magnetic highs that are predominantly oriented NNW (Fig. 2b). Bouguer gravity values are relatively high over the Wonnaminta Zone (Figs. 2a and 4a).

The seismic reflection image of the Wonnaminta zones shows that the non-reflective to poorly reflective crust exists down to the Moho (~35 km depth or ~12 seconds TWT; Fig. 4d). The poor reflection packages of the Wonnaminta Zone have been thrust over the Bancannia Trough by the east dipping Lawrence Fault. The central part of the Wonnaminta Zone is characterized by an antiformal stacking and a series of northeast dipping reverse

ACCEPTED MANUSCRIPT

faults (Fig. 4d). The relatively high Bouguer gravity corresponds to this the antiformal stacking at depth (Fig. 4a, d), and the short-intense aeromagnetic data possibly correspond to the faults (Fig. 4b, d). To the east of the Wonnaminta Zone, the Koonenberry Fault is characterized by a relatively wide shear zone indicated by parallel to semi-parallel reflection packages that extend down to Moho at dip of ~ 40° southwest (Fig. 4d). The kinematics along the Koonenberry Fault cannot be interpreted from the seismic data, but previous authors have interpreted it as a reverse fault (Mills and David, 2004; Greenfield et al., 2011).

4.1.3. Kayrunnera Zone

The RTP aeromagnetic and Bouguer gravity images (Fig. 2a, b) show a relative decrease in both magnetic intensity and density from the Wonnaminta Zone to the Kayrunnera Zone. The NNW-trending Koonenberry Fault is the boundary between these two zones (Fig. 2b). The decreased gravity and short-wavelength linear to curvilinear magnetic anomalies over the Kayrunnera Zone (Fig. 4a, b) possibly corresponds to folded metasedimentary rocks at depth.

Seismic interpretation (Fig. 4d) across the Kayrunnera Zone shows that, in comparison to the western part, the Moho occurs at slightly shallower depth. The crust extends down to ~35 km depth and shows similar reflection properties to those beneath the Bancannia Trough and the Wonnaminta Zone. At the eastern limit of the seismic transect, the Kayrunnera Zone is characterized by a relatively strong reflection packages dipping almost parallel to the Koonenberry Fault Zone. The nature of this crustal structure is not clear due to the relatively low seismic resolution and lack of kinematic indicators. Beneath this structure, the crust is characterized by a number of southwest dipping, weak, parallel to sub-parallel reflectors.

4.1.4. Northwestern Koonenberry Belt

The potential field anomalies of the Koonenberry Belt become less intense towards the northwest (Fig. 5). The magnetic signature in this area is characterized by very low amplitude smooth anomalies (Fig. 5a), which likely correspond to sedimentary rocks (i.e., Late Cambrian Lycosa Formation) of the Warburton Basin beneath the Permian to Triassic sedimentary rocks of the Cooper Basin (Sun and Gravestock, 2001). A prominent curvature of broad gravity low (Fig. 5b) is marked by an ~ENE trending curvilinear lineament and in weak traces of tilt derivate of (500m) upward continuation of RTP data (Fig. 5c, d). A

ACCEPTED MANUSCRIPT

number of low to moderate amplitude irregular shaped magnetic bodies correspond to lower gravity are interpreted as granitic intrusions in to the basement (Fig. 5a, b, e).

4.3. Western part of the southern Thomson Orogen

4.3.1. Olepoloko Fault and associated structures

The Olepoloko Fault is located to the east of the Kayrunnera Zone and marks the boundary between the Koonenberry Belt (i.e., the Delamerian Orogen) and the southern Thomson Orogen (Fig. 2b). To the south of the Olepoloko Fault, a broad gravity low characterizes the Nelyambo Trough, which is considered to be part of the Lachlan Orogen (Fig. 2a). In contrast with the aeromagnetic signature north of Olepoloko Fault, the Nelyambo Trough is characterized by a smooth and relatively low aeromagnetic response (Figs. 2b and 6a).

Figure 6c shows an interpreted composite image of RTP aeromagnetic data over tilt derivative of 500m upward continuation of RTP aeromagnetic data. This image highlights two faults (Torowoto and Tongo faults) sub-parallel to the Olepoloko Fault (Fig. 6c). Structural interpretation of tilt derivatives of RTP data (Fig. 7b) shows that a number of magnetic anomalies are dragged towards the fault with an apparent sinistral sense of movement and offset by few ~E-W trending minor faults. The faults merge with the Torowoto and Tongo faults at a low angle (less than 30°). These minor faults can be interpreted as synthetic Riedel shears associated with the (likely sinistral) Torowoto and Tongo faults. The Torowoto and Tongo faults also merge at low-angle with the Olepoloko Fault (Figs. 6c and 7b), possibly suggesting that these two faults are synthetic Riedel shears/faults of the Olepoloko Fault. The Olepoloko and Torowoto faults are cut at relatively high angle and dextrally offset ~2 km by the ~NNW trending Purnanga Fault (Fig. 7b), which is either an antithetic Riedel shear of the Olepoloko Fault or a younger fault.

Interpretation of seismic transects (05GA TL 1 and 05GA TL 2, Fig. 8) shows that the north-dipping Olepoloko Fault separates a thicker crust of the Thomson Orogen from relatively thinner crust of the Lachlan Orogen. The Moho is characterized by very strong and continuous reflector at ~30 km depth (~10.5 seconds TWT) to the south of the Olepoloko Fault and ~40-45 km (~15 seconds TWT) to the north.

The Lachlan Orogen is located to the south of the Olepoloko fault and is characterized by distinctive reflective lower crust (~ 6.5 to 10.5 seconds TWT) and non-reflective upper crust (~2 to 6.5 seconds TWT) (Fig. 8). Glen et al. (2013) suggested that the weakly reflective

ACCEPTED MANUSCRIPT

upper crust may represent Ordovician turbidites. Above the upper crust, wedge-shaped reflection packages have been identified at ~1-3 seconds TWT (Fig. 8b). These wedges are representative of fault-bounded half-graben, possibly of syn-rift packages that are equivalent to the Late Silurian – Early Devonian Cobar Supergroup (Glen et al., 2013). A number of faults within this syn-rift package were subjected to inversion, because these faults cut and offset the top of syn-rift unconformity and younger sedimentary rocks (Fig. 8b). Few small reverse fault are also present within the upper part of the non-reflective crust.

A package of gently onlapping reflectors overlays the rift-packages. These parallel to subparallel strong reflectors are representative of the Middle to Late Devonian Mulga Downs Group (Glen et al., 2013). The refection packages associated with these two units (Cobar Supergroup and Mulga Downs Group) are terminated against the Olepoloko Fault, indicating that the youngest movement along the Olepoloko Fault took place after the deposition of the Middle to Late Devonian successions. The thickness of the Middle to Late Devonian succession gradually increases southward (Fig. 8b). Farther south, this unit is thinned and uplifted by a south-dipping inverted normal fault (i.e., the Mountain Jack Fault) (Fig. 8b). The syn-rift half-graben indicates that the fault was a normal fault during Late Silurian to Early Devonian and was inverted following the deposition of the Middle to Late Devonian sediments. The onlapping growth strata of the Middle to Late Devonian packages above the syn-rift unconformity suggest that the reactivation of the Mountain Jack Fault took place during sedimentation.

To the north of the Olepoloko Fault, the thicker reflective lower crust of the Thomson Orogen is characterized by a relatively weaker seismic impedance compared to the Lachlan lower crust (Fig. 8). A series of relatively strong and more continuous south-dipping reflection package can be identified at ~8 to 10 seconds TWT. This package is overprinted by a relatively steeply dipping reverse fault, which merges with the Olepoloko Fault at depth. A number of smaller faults can be identified based on displacement and reflection geometry of the form lines. These faults are predominantly dipping northward. The overall geometry of the Olepoloko Fault and its associated structures suggests that it is a primary structure within a positive flower structure (Fig. 8).

The upper non-reflective crust of the Thomson Orogen is characterized by a similar reflection configuration as of the Lachlan upper crust. Separation of the reflectors at the base and top of the non-reflective lower crust indicates that the estimated reverse vertical throw on the Olepoloko Fault is possibly greater than 7 km. The Late Silurian – Early Devonian rift-

ACCEPTED MANUSCRIPT

package and Middle to Late Devonian parallel to subparallel reflectors are completely absent to the north of Olepoloko Fault (Fig. 8b). The Middle to Late Devonian packages are separated from the Mesozoic to Cenozoic younger cover by a major erosional surface, which can be identified by a relatively strong high amplitude reflector (Fig. 8a). This unconformity also extends to the north of the Olepoloko fault and shows no movement of the Olepoloko Fault (Fig. 8b).

4.3.2. Mount Oxley Fault

Mount Oxley Fault is sub-parallel to the Olepoloko Fault (Figs. 2b and 6c). Seismic imaging (Fig. 8b) across the fault shows that this is a reverse fault dipping opposite to the Olepoloko Fault. Moderate to weak reflectors of the reflective lower crust of the Thomson Orogen are offset by this fault, showing ~2-3 km of vertical displacement.

In between the Olepoloko and Mount Oxley faults, a zone of relatively high amplitude linear to irregular shaped magnetic bodies has been identified (Fig. 6c). These magnetic bodies are interpreted to be associated with the Late Silurian (~422 Ma) Louth Volcanics (Glen et al., 2010) (Figs. 3 and 6d). Tilt-derivative of the RTP aeromagnetic data of the Louth Volcanics shows folded structural trends with a ~NE-SW axial surface (Fig. 7c, d). To the east, a small segment of the Louth Volcanics is dextrally offset ~25 km by the Mount Oxley Fault (Fig. 7c, d).

4.3.3. Willara Fault and Kulkyne Fracture Zone

To the north of Mount Oxley Fault, a large area of a relative magnetic low characterizes the Early Devonian Hungerford Granite (Figs. 6d and 7f). Two ~WNW trending faults (Kulkyne Fracture Zone and Willara Fault) cut the granite. The distance between the two faults is ~50 km. The interpretation of the tilt derivatives of the RTP of this granite shows a sigmoidal shaped magnetic feature (blue dashed lines in Fig. 7f). This sigmoidal shape seems to have been dragged towards the Kulkyne Fracture Zone and Willara Fault with an apparent sinistral sense of movement (Fig. 7f).

4.3.4. Unnamed faults F1 and F2

ACCEPTED MANUSCRIPT

The interpretation of geophysical images shows that the northern extent of the southern Thomson Orogen is defined by a ~300 km long geophysical expression, trending ~WNW (Fig. 5). Bouguer gravity data show that this geophysical feature follows a ~50 km wide belt of gravity low (Fig. 5b). A number of semi-rounded to irregular shaped granitic bodies can be identified along this belt (Fig. 5e).

To the north of the gravity low, the structural trends interpreted from the aeromagnetic images (Figs. 5d and 9b) are cut-off by a linear ~WNW trending structure. This linear structure is associated with dextrally offset (~25 km) magnetized bodies and is therefore interpreted as a fault (hereinafter F1) (Fig. 9b). Another relatively high magnitude magnetic body was dragged and offset dextrally by a smaller ~NW-trending fault (hereinafter F2), which terminates against F1 at a low angle (Fig. 9b). Both faults show evidence of dextral kinematics. The dextral kinematics, together with the relatively low angle (less than 30°) between F1 and F2, may suggest that F2 is a synthetic Riedel shear associated with a larger dextral fault (F1). Farther southeast, the F1 fault merges with the Niccamucca Fault, which has a similar ~WNW trend (Figs. 2b and 10c). This fault cuts and dextrally offsets a highly magnetized granitic body (Fig. 10c, d). The Niccamucca Fault terminates against the western part of Culgoa Fault farther east (Fig. 10c).

4.4. Eastern part of the southern Thomson Orogen

4.4.1. Louth-Eumarra Shear Zone and associated structures

The RTP aeromagnetic image of the eastern part of the southern Thomson Orogen shows a series of moderate to high amplitude long-wavelength magnetic bodies surrounded by low amplitude anomalies (Fig. 10a). The area is characterized by a number of ~E-W trending major faults, such as the Louth-Eumarra Shear Zone, Boomi Fault, Little Mountain Fault, and Culgoa Fault (Fig. 10c).

The Louth-Eumarra Shear Zone (Fig. 2b and 10c) is a broad ~E-W trending geophysical feature that follows a similar trend as the Olepoloko Fault. Detailed structural and kinematic analysis of this part of the southern Thomson Orogen, recently presented by Dunstan et al. (2016), shows a substantial component of dextral kinematics. To the north, the shear zone is marked by an ~E-W trending structure, named Boomi Fault (Fig. 10c). Interpretation of the tilt derivative image of aeromagnetic data shows that moderate to high amplitude magnetic bodies (Fig. 10a, c) were dragged dextrally by the Louth-Eumarra Shear Zone and Boomi

ACCEPTED MANUSCRIPT

Fault. These magnetic bodies are inferred to be related to Late Silurian – Early Devonian igneous intrusions (Tarcoon Complex) (Fig. 10d).

To the east of the Louth-Eumarra Shear Zone, high amplitude ~N-S-trending magnetic bodies may correspond to the northern extension of the Ordovician Macquarie Arc (Fig. 10a, d). A series of ~EW to ENE trending dextral faults dragged and offset these magnetic bodies (F4, F5, F6 and F7, Fig. 10c). Regional Bouguer gravity map shows that a ~N-S-oriented high-gravity body has been cut and dragged by an ~E-W trending lineament that may correspond to the Louth-Eumarra Shear Zone (Fig. 2a).

The Little Mountain Fault is located in between the Olepoloko Fault and Louth-Eumarra Shear Zone (Fig. 10c). This is an ~ENE trending fault, which may represent the westward extension of the Louth-Eumarra Shear Zone.

4.4.2. Culgoa Fault

The Culgoa Fault is marked by a narrow ~ENE trending gravity and magnetic high that may correspond to ultramafic intrusions along the fault zone (Figs. 2a, b and 10c). Interpretation of aeromagnetic data shows a folded magnetic feature northeast of the Culgoa Fault (Fig. 10c). This folded feature is bounded by another fault, which trends parallel to the Culgoa Fault (Fig. 10c). The sigmoidal shape of this ~NNE-SSW trending magnetic body indicates possible dextral kinematics along the Culgoa Fault.

In seismic transect DMR 98-02 (Fig. 11), the Culgoa Fault is a north-dipping reverse fault. A weakly reflective package similar to the non-reflective upper crust of the Thomson Orogen (Fig. 8) can be identified in the northern part of the section that was uplifted by the reverse motion of the Culgoa Fault (Fig. 11). Few smaller second order faults are also present within the non-reflective package. To the south of the Culgoa Fault, a zone of strong parallel to sub-parallel reflectors is onlapping above the non-reflective upper crust, thinning towards the south (Fig. 11). The overall reflection geometry of this package can be interpreted as syn-kinematic growth-strata developed due to reverse movement of the Culgoa Fault. Above this onlapping growth-strata, reflectors are parallel with fair continuity. Borehole information from Brewarrina 1 suggests that this package corresponds to Middle Devonian sedimentary rocks (Carty and Moffitt, 2001). The borehole did not intersect the underlying onlapping reflectors. We interpret that these reflectors to represent Middle Devonian or older sedimentary rocks. The parallel reflectors above the syn-kinematic growth-strata may

ACCEPTED MANUSCRIPT

indicate that deformation ceased during the deposition of this Middle Devonian succession. Both packages are folded and affected by a series of south-dipping reverse faults with a minor displacement located in between CDP 3000-4000, indicating that another episode of contractional deformation possibly took place after the deposition of the Middle Devonian sedimentary rocks. Another small reverse fault can be identified at the southern part of the line (Fig. 11). A prominent angular unconformity can be identified at ~0.5 seconds, between relatively undeformed younger successions and deformed older rocks.

4.4.3. Unnamed Fault F3

To the west of Nebine Ridge, a belt of narrow magnetic linear features (Figs. 5a and 9c) are dextrally dragged and offset by an ~ENE to ~NE trending fault (hereinafter F3), which terminates against the F1 fault at a high angle. These magnetic bodies correspond to the metasedimentary rocks of the Werewilka Formation (Fig. 5f). The age of the Werewilka Formation is unknown; however, xenoliths of this formation were found in the 463 ± 11 Ma Granite Springs Granite (Cross et al., 2015), indicating that the age of the metasedimentary rocks is older than Late Ordovician.

5. DISCUSSION

5.1. Timing and kinematics of faults in the southern Thomson Orogen

The interpretation of potential field and 2D deep seismic datasets reveals that a series of faults occur parallel to the curvilinear ~E-W geophysical trend of the southern Thomson Orogen. Based on the interpretation of gridded aeromagnetic images, it seems that many of these faults have involved a strike-slip component with evidence for dextral, sinistral and oblique kinematics. Activity along these faults may reflect multiple phases of deformation and fault generation or reactivation that possibly started from the Delamerian Orogeny (Fig. 12). However, the timing of deformation is unfortunately poorly constrained, and in particular, it remains unclear whether the abovementioned major structures were already active during the Delamerian Orogeny (~500 Ma), or whether they only reflect later (e.g., Benambran and Tabberabberan) deformation.

Deformation associated with Delamerian Orogeny is recorded in both the Koonenberry Belt and in exposures of the Thomson Orogen in northeastern Queensland (Anakie, Charters

ACCEPTED MANUSCRIPT

Towers and Greenvale provinces) (Figs. 1a and 3). These ostensibly disparate areas could potentially be connected through the subsurface basement geology of the southern Thomson Orogen. Nonetheless, the age of the Southern Thomson basement remains poorly constrained with no robust evidence supporting the existence of Cambrian or Precambrian rocks under the sedimentary cover. The only direct evidence for the existence of a pre-Delamerian basement is the ~577 Ma U-Pb zircon ages from the Warraweena Volcanics, which were interpreted by Glen et al. (2013) as representing magmatic ages [however, see Burton and Trigg (2014) for an alternative interpretation]. The interpretation of Glen et al. (2013) implies that the Southern Thomson Orogen includes a Neoproterozoic basement.

In the Koonenberry Belt, crustal-scale reverse faults are considered to represent Delamerian deformation (Greenfield et al., 2010; Greenfield et al., 2011). If the southern Thomson Orogen is indeed underlain by a Neoproterozoic basement, it is potentially possible that the eastward continuation of the Koonenberry Belt (i.e., the Delamerian Orogen) is represented by some of the major structures discussed in this paper (Fig. 12a). Glen et al. (2013) have also suggested that the Olepoloko Fault separates Neoproterozoic to earliest Cambrian basement rocks (in the southern Thomson Orogen) from younger (Ordovician to Devonian) rocks of the Lachlan Orogen. The maximum age constraint for the development of the Olepoloko Fault, at ~500 Ma, could potentially be consistent with the timing of Delamerian deformation. However, given the lack of direct evidence supporting Delamerian deformation in the southern Thomson Orogen, the kinematic scenario shown in Figure 12a remains speculative.

Along the eastern part of the boundary between the Thomson and Lachlan orogens, the Louth-Eumarra Shear Zone (including Boomi Fault and faults F3 – F7) shows clear evidence for dextral kinematics (Figs. 9d and 10b), with the Culgoa Fault also displaying evidence for a reverse motion (Fig. 11). The Late Silurian to Early Devonian Tarcoon Pluton Complex is deformed by the Louth-Eumarra Shear Zone (Dunstan et al., 2016), indicating that at least a component of the described dextral motion took place during or after the Late Silurian to Early Devonian emplacement of these igneous complex. Dunstan et al. (2016) hypothesized that the Late Silurian to Early Devonian deformation along the Louth-Eumarra Shear Zone may correspond to the reactivation of pre-existing crustal-scale structures. For example, a change in the structural orientation, from ~N-S to ~NE-SW at the Kenilworth area and Brevelon Tank site (Fig. 10b, c), may correspond to dextral strike-slip faulting along the Louth-Eumarra Shear Zone associated with Benambran Orogeny (Dunstan et al., 2016).

ACCEPTED MANUSCRIPT

Similarly, the Late Silurian Louth Volcanics (Fig. 7d) shows folds trending ~NE-SW that possibly correspond to dextral movement along the Mount Oxley and Olepoloko faults during the latest Benambran Orogeny or Tabberabberan Orogeny. The timing of movement along F1 to F7 (Figs. 5d and 10b) is not constrained. However, the dextral kinematics along these faults may imply coeval deformation.

Evidence for younger reactivation is also recognized along the Olepoloko Fault. The seismic transect across the Olepoloko Fault shows an almost equal thickness of the Ordovician packages on both sides of the fault (Fig. 8) and an absence of Silurian-Devonian rocks north of the Olepoloko Fault (the hanging wall block). These stratigraphic relationships indicate that reverse movement along the fault resulted in significant uplift and erosion of this block. The onlapping configuration of the Middle to Late Devonian strata, and the evidence for minor inversion of normal faults (Fig. 8) in the Lachlan Orogen, suggest that at least one episode of major reverse movement took place during or after Middle to Late Devonian.

The broad positive flower-like structure (Fig. 8b) in the southern Thomson Orogen indicates possible transpressional setting (Harding, 1985; Woodcock and Fischer, 1986; Woodcock and Rickards, 2003). The kinematic analysis of the Olepoloko Fault and associated faults (Tongo, Torowoto and other minor sinistral faults) suggests that the fault was possibly subjected to sinistral movement (Fig 7b). Evidence for sinistral displacement can also be interpreted in between the Willara Fault and Kulkyne Fractures (Fig. 7f). The 419.5 ± 2.5 Ma Hungerford Granite (Bultitude and Cross, 2012), located in between these two faults, provides a maximum constraint for sinistral movement along these faults (Fig. 7f).

Seismic interpretation across the Culgoa Fault (Fig. 11) shows evidence for two possible phases of reverse movement. The deposition of onlapping growth strata (Middle Devonian or older) possibly corresponds to the ~390-380 Ma Tabberabberan Orogeny. Folding of both parallel reflection package (i.e., Middle Devonian sediments) and underlying growth-strata suggest that younger reactivation took place after Middle Devonian possibly corresponding to the ~360-340 Ma Kanimblan Orogeny.

In summary, the development of major fault systems in the southern Thomson Orogen may have initiated during the Delamerian Orogeny (Fig. 12a). The observed dextral kinematics along major faults in this area was likely triggered by ~E-W contraction associated with Benambran deformation (Fig. 12b). Subsequently, ~E-W Tabberabberan contraction was possibly responsible for further fault reactivation (Fig. 12c). The Tabberabberan deformation

ACCEPTED MANUSCRIPT

may have been responsible for the initiation of sinistral faults along the western part of the Olepoloko Fault (Fig. 12c). Evidence for Kanimblan deformational event can also be observed along the Culgoa Fault.

5.2. Tectonic implications

Our results show that an arrangement of curvilinear ~E-W structures (Olepoloko Fault and Louth Eumarra Shear Zone) separate the thicker southern Thomson crust from the thinner crust of the Lachlan Orogen (Fig. 8). Seismic tomographic studies (Fig. 13) show that the Thomson and Delamerian orogens, in contrast with the Lachlan Orogen, are characterized by higher seismic velocities (Kennett et al., 2004; Rawlinson and Kennett, 2008; Kennett et al., 2013; Rawlinson et al., 2015). Teleseismic data from the WOMBAT transportable array [see Figure 2.9 in Rawlinson et al. (2015)] show a similar characteristic of high velocity lithosphere beneath both the Delamerian and southern Thomson orogens and a significantly different lithosphere beneath the Lachlan Orogen. The high velocity lithosphere of the Thomson and Delamerian orogens corresponds to thicker (and possibly older) lithosphere compared to that of the Lachlan Orogen (Rawlinson et al., 2015). A N-S section constructed from the teleseismic model [see Figure 2.9 in Rawlinson et al. (2015)] shows that a north-dipping lithospheric structure exists at the southern Thomson Orogen, separating the high velocity lithosphere of Thomson Orogen from the relatively lower velocity lithosphere of the Lachlan Orogen.

The Delamerian crust beneath the northeastern part of Kayrunnera Zone (Fig. 4) shows southwest-dipping, moderately strong, parallel to sub-parallel reflectors. The reflective lower crust of the Thomson Orogen also exhibits similar reflection configuration dipping south (Fig. 8). This comparison indicates that the crust beneath these two tectonic blocks might be of the same origin. As discussed in the previous section, Glen et al. (2013) hypothesized that the origin of the thicker crust beneath the southern Thomson Orogen is associated with a sliver of older (Neoproterozoic) crust (Fig. 14). This hypothesis is supported by the teleseismic model of Rawlinson et al. (2015).

Across the central Thomson Orogen, in contrast, seismic data show a thinner, extended substrate crust that may represent extended continental crust (Finlayson et al., 1990; Glen, 2005; Spampinato et al., 2015b) or even oceanic crust (Glen et al., 2013). The thinner

ACCEPTED MANUSCRIPT

substrate crust at the central part of the Thomson Orogen could have formed by rifting in the Early Cambrian (Glen, 2005; Fergusson et al., 2009; Glen, 2013; Glen et al., 2013).

The significant contrast in crustal and lithospheric characteristics between the Thomson and Lachlan orogens may suggest that different geodynamic processes shaped the two major segments of the Tasmanides (i.e., the northern segment north of the Thomson-Lachlan boundary and the southern segment south of it). While the northern Tasmanides display little change in the location of the magmatic arc between the Ordovician and Permian, the southeastern Tasmanides show spatio-temporal variations in the occurrence of arc magmatism (Fig. 14). Thus, the southern segment of the Tasmanides was likely controlled by a relatively mobile plate boundary. Furthermore, the occurrence of oroclinal structures only south and east of the Thomson Orogen (Fig. 14) (Musgrave, 2015), and the possible genetic link between oroclines and plate boundary migration (Moresi et al., 2014; Rosenbaum, 2014) support the suggestion that segmentation of the Tasmanides was controlled by along-strike variations in the subduction zone. Segmentation of convergent plate boundaries through the development of orogen-perpendicular lithospheric structures is recognized in modern tectonics (e.g., Caribbean-South American Plate margin; Govers and Wortel, 2005; Miller and Becker, 2012), and it is likely that similar processes have played a major role during the development of Paleozoic eastern Australia.

The timing of segmentation between the northern and southern Tasmanides is largely unknown. Dunstan et al. (2016) have suggested that along-strike variations in the rates of trench retreat have already took place in the Early to Middle Cambrian, giving rise to back-arc extension in the northern Tasmanides and crustal thinning in the central Thomson Orogen (Glen, 2005; Glen et al., 2013). According to the this tectonic scenario, the ~E-W structures in the southern Thomson Orogen (including the Olepoloko Fault and Louth-Eumarra Shear Zone) initiated in response to tearing and crustal segmentation between the northern and southern segments of the Tasmanides, thus explaining the similarities between Delamerian deformation in the Koonenberry Belt and the Anakie Inlier of the northeast Thomson Orogen.

6. CONCLUSION

Interpretation of geophysical datasets from the boundary between the Thomson Orogen and the Delamerian and Lachlan orogens reveals crustal-scale curvilinear ~E-W structural features that are controlled by a number of fault systems. Fault kinematic indicators show

ACCEPTED MANUSCRIPT

dextral, sinistral and reverse motions, indicating multi-phase reactivation history of these structures. The timing of activity of the major crustal-scale structure (e.g., Olepoloko Fault and Louth-Eumarra Shear Zone) is not well constrained but is consistent with the timing of Delamerian Orogeny and subsequent reactivation events (Fig. 12). The origin of the ~E-W structures of the Thomson-Lachlan boundary may have resulted from lithospheric segmentation within the Tasmanides in response to along-strike plate boundary variations.

Acknowledgement

This research is funded by the Australian Research Council Grant LP140100874. TMI aeromagnetic, Bouguer gravity and seismic datasets were obtained from Geoscience Australia, Geological Survey of Queensland, Geological Survey of New South Wales and Geological Survey of South Australia. We are also grateful to the Research School of Earth Sciences, The Australian National University, for providing a permission to use the AuSREM mantle model. We thank P. Betts and an anonymous reviewer for their constructive comments, and Rosemary Hegarty, David Purdy, Uri Shaanan and Abbas Babaahmadi for support and assistance.

References

Betts, P.G., Valenta, R.K., Finlay, J., 2003. Evolution of the Mount Woods Inlier, northern Gawler Craton, Southern Australia: an integrated structural and aeromagnetic analysis. Tectonophysics 366, 83-111.

Black, L.P., 2006. SHRIMP U–Pb zircon ages obtained during 2005/06 for NSW Geological Survey projects. Geological Survey of New South Wales, GS 2006/821 (unpubl.).

Black, L.P., 2007. SHRIMP U–Pb zircon ages obtained during 2006/07 for NSW Geological Survey projects. Geological Survey of New South Wales, GS 2007/298 (unpubl.).

Blevin, P., 2011. Petrological, chemical and metallogenic notes on the granites of the Bourke 250000 sheet, NSW. Geological Survey of New South Wales, GS2011/0624.

Bodorkis, S., Blevin, P.L., Bruce, M.C., Gilmore, P.J., Glen, R.A., Greenfield, J.E., Hegarty, R., Percival, I.G., Quinn, C.D., 2013. New SHRIMP U–Pb zircon ages form the Lachlan, Thomson and Delamerian orogens. New South Wales, Geoscience Australia Record 2013/0427.

Bultitude, R., Cross, A., 2012. Granites of the Eulo Ridge. In: Jell, P. (Ed.), Geology of Queensland. Geological Survey of Queensland, Brisbane, pp. 166-167.

Burton, G.R., 2010. New structural model to explain geophysical features in northwestern New South Wales: Implications for the tectonic framework of the Tasmanides. Australian Journal of Earth Sciences 57, 23-49.

ACCEPTED MANUSCRIPT

Burton, G.R., Campbell, L.M., Gerakiteys, C.L., Percival, I.G., Robson, D.F., Trigg, S.J., 2012. Sussex and Byrock 1:100,000 Geological Sheets 8135 and 8136: Explanatory Notes. Geological Survey of New South Wales, Report Number - 1742564054.

Burton, G.R., Trigg, S.J., 2014. Geodynamic significance of the boundary between the Thomson Orogen and the Lachlan Orogen, northwestern New South Wales and implications for Tasmanide tectonics: discussion. Australian Journal of Earth Sciences 61, 639-641.

Carty, C.J., Moffitt, R.S., 2001. Well completion report DM Brewarrina DDH-1/1A. Geological Survey of New South Wales, GA 2001/419.

Cas, R.A., 1983. Paleogeographic and Tectonic Development of the Lachlan Fold Belt Southeastern Australia. Special Publication Geological Society of Australia 10, 104.

Cawood, P.A., Pisarevsky, S.A., Leitch, E.C., 2011. Unraveling the New England orocline, east Gondwana accretionary margin. Tectonics 30, TC5002, doi: 10.1029/2011TC002864.

Collins, W.J., 2002. Hot orogens, tectonic switching, and creation of continental crust. Geology 30, 535-538.

Coney, P.J., Edwards, A., Hine, R., Morrison, F., Windrim, D., 1990. The regional tectonics of the Tasman orogenic system, eastern Australia. Journal of Structural Geology 12, 519-543.

Cooper, G.R.J., Cowan, D.R., 2005. Differential reduction to the pole. Computers & Geosciences 31, 989-999.

Cross, A., Dunkley, D., Bultidude, R., Brown, D., Purdy, D., Withnall, I., von Gnielinski, F., Blake, P., 2015. Summary of results Joint GSQ-GA geochronology project: Thomson Orogen, New England Orogen and Mount Isa region, 2010-2012. Queensland Geological Record 2015/01.

Draper, J.J., 2006. The Thomson Fold Belt in Queensland revisited. ASEG Extended Abstracts 2006, 1-6.

Dunstan, S., Rosenbaum, G., Babaahmadi, A., 2016. Structure and kinematics of the Louth-Eumarra Shear Zone (north-central New South Wales, Australia) and implications for the Paleozoic plate tectonic evolution of eastern Australia. Australian Journal of Earth Sciences 63, 63-80.

Fergusson, C.L., 1991. Thin-skinned thrusting in the northern New England Orogen, central Queensland, Australia. Tectonics 10, 797-806.

Fergusson, C.L., 2009. Tectonic evolution of the Ordovician Macquarie Arc, central New South Wales: Arguments for subduction polarity and anticlockwise rotation. Australian Journal of Earth Sciences 56, 179-193.

Fergusson, C.L., Carr, P.F., Fanning, C.M., Green, T.J., 2001. Proterozoic–Cambrian detrital zircon and monazite ages from the Anakie Inlier, central Queensland: Grenville and Pacific-Gondwana signatures. Australian Journal of Earth Sciences 48, 857-866.

Fergusson, C.L., Gray, D.R., Cas, R.A., 1986. Overthrust terranes in the Lachlan fold belt, southeastern Australia. Geology 14, 519-522.

Fergusson, C.L., Henderson, R., Blake, P., Bultidude, R., Champion, D., Cross, A., Draper, J., Green, T.J., Hutton, L., Jell, P.A., 2013. Thomson orogen. In: Jell, P.A. (Ed.), Geology of Queensland. Geological Survey of Queensland, Brisbane, pp. 113-224.

Fergusson, C.L., Henderson, R.A., Fanning, C.M., Withnall, I.W., 2007. Detrital zircon ages in Neoproterozoic to Ordovician siliciclastic rocks, northeastern Australia: implications for the tectonic history of the East Gondwana continental margin. Journal of the Geological Society of London 164, 215-225.

ACCEPTED MANUSCRIPT

Fergusson, C.L., Offler, R., Green, T., 2009. Late Neoproterozoic passive margin of East Gondwana: Geochemical constraints from the Anakie Inlier, central Queensland, Australia. Precambrian Research 168, 301-312.

Finlayson, D.M., 1993. Crustal architecture across Phanerozoic Australia along the Eromanga-Brisbane Geoscience Transect: Evolution and analogues. Tectonophysics 219, 191-211.

Finlayson, D.M., Leven, J.H., 1987. Lithospheric structures and possible processes in Phanerozoic eastern Australia from deep seismic investigations. Tectonophysics 133, 199-215.

Finlayson, D.M., Leven, J.H., Etheridge, M.A., 1988. Structural styles and basin evolution in Eromanga region, eastern Australia. AAPG Bulletin 72, 33-48.

Finlayson, D.M., Wake-Dyster, K.D., Leven, J.H., Johnstone, D.W., Murray, C.G., Harrington, H.J., Korsch, R.J., Wellman, P., 1990. Seismic imaging of major tectonic features in the crust of Phanerozoic eastern Australia. Tectonophysics 173, 211-230.

Foden, J., Elburg, M.A., Dougherty-Page, J., Burtt, A., 2006. The timing and duration of the Delamerian Orogeny: correlation with the Ross Orogen and implications for Gondwana assembly. The Journal of Geology 114, 189-210.

Foster, D.A., Gray, D.R., 2000. Evolution and structure of the Lachlan Fold Belt (Orogen) of eastern Australia. Annual Review of Earth and Planetary Sciences 28, 47-80.

Fraser, G.L., Gilmore, P., Fitzherbert, J.A., Trigg, S.J., Campbell, L.M., Deyssing, L., Thomas, O.D., Burton, G.R., Greenfield, J.E., Blevin, P.L., Simpson, C.J., 2014. New SHRIMP U-Pb zircon ages from the Lachlan, southern Thomson and New England orogens, New South Wales. Geoscience Australia Record 2014/053.

Gibert, D., Galdeano, A., 1985. A computer program to perform transformations of gravimetric and aeromagnetic surveys. Computers & Geosciences 11, 553-588.

Glen, R.A., 1992. Thrust, extensional and strike-slip tectonics in an evolving Palaeozoic orogen—a structural synthesis of the Lachlan Orogen of southeastern Australia. Tectonophysics 214, 341-380.

Glen, R.A., 2005. The Tasmanides of eastern Australia. In: Vaughan, A.P.M., Leat, P.T., Pankhust, R.J. (Eds.), Terrane processes at the margins of Gondwana. Geological Society, London, Special Publications, 246, pp. 23-96.

Glen, R.A., 2013. Refining accretionary orogen models for the Tasmanides of eastern Australia. Australian Journal of Earth Sciences 60, 315-370.

Glen, R.A., Clare, A., Spencer, R., 1996. Extrapolating the Cobar Basin model to the regional scale: Devonian basin-formation and inversion in western New South Wales. In: Cook, W.G., Ford, A.J.H., McDermott, J.J., Standish, P.N., Stegman, C.L., Stegman, T.M. (Eds.), The Cobar Mineral Field - A 1996 prospective. Vic: Australian Institute of Mining and Metallurgy, Melbourne, pp. 43-84.

Glen, R.A., Djomani, Y.P., Belousova, E., Hegarty, R., Korsch, R.J., 2014. Geodynamic significance of the boundary between the Thomson Orogen and the Lachlan Orogen, northwestern New South Wales and implications for Tasmanide tectonics: reply. Australian Journal of Earth Sciences 61, 643-657.

Glen, R.A., Korsch, R.J., Direen, N.G., Jones, L.E.A., Johnstone, D.W., Lawrie, K.C., Finlayson, D.M., Shaw, R.D., 2002. Crustal structure of the Ordovician Macquarie Arc, Eastern Lachlan Orogen, based on seismic-reflection profiling. Australian Journal of Earth Sciences 49, 323-348.

Glen, R.A., Korsch, R.J., Hegarty, R., Saeed, A., Djomani, Y.P., Costelloe, R.D., Belousova, E., 2013. Geodynamic significance of the boundary between the Thomson Orogen and the Lachlan Orogen, northwestern New South Wales and implications for Tasmanide tectonics. Australian Journal of Earth Sciences 60, 371-412.

ACCEPTED MANUSCRIPT

Glen, R.A., Saeed, A., Hegarty, R., Percival, I.G., Bodorkos, S., Griffin, W.L., 2010. Preliminary zircon data & tectonic framework for the Thomson Orogen, northwestern NSW. Geological Survey of New South Wales, GS 2010/0379 (unpubl.)

Govers, R., Wortel, M.J.R., 2005. Lithosphere tearing at STEP faults: Response to edges of subduction zones. Earth and Planetary Science Letters 236, 505-523.

Gray, D.R., Foster, D.A., 1997. Orogenic concepts; application and definition; Lachlan fold belt, eastern Australia. American Journal of Science 297, 859-891.

Greenfield, J.E., Musgrave, R.J., Bruce, M.C., Gilmore, P.J., Mills, K.J., 2011. The Mount Wright Arc: a Cambrian subduction system developed on the continental margin of East Gondwana, Koonenberry Belt, eastern Australia. Gondwana Research 19, 650-669.

Greenfield, J.E., P.J, G., Mills, K.J., 2010. Explanatory notes for the Koonenberry Belt geological maps. Geological Survey of New South Wales Bulletin 35, 1-528.

Gunn, P.J., Maidment, D., Milligan, P.R., 1997. Interpreting aeromagnetic data in areas of limited outcrop. AGSO Journal of Australian Geology and Geophysics 17, 175-186.

Harding, T.P., 1985. Seismic characteristics and identification of negative flower structures, positive flower structures, and positive structural inversion. AAPG Bulletin 69, 582-600.

Hegarty, R., 2010. Preliminary geophysical–geological interpretation map of the Thomson Orogen. Release of Provisional and Preliminary Information (DVD) Geological Survey of New South Wales, Department of Industry & Investment, Maitland.

Hegarty, R., 2011. Bourke 1:250 000 Geophysical-Geological Interpretation Map, SH/55-10. Geological Survey of New South Wales, Maitland.

Henderson, R.A., 1983. Early Ordovician faunas from the Mount Windsor subprovince, northeastern Queensland. Memoirs of the Association of Australasian Palaeontologists 1, 145-175.

Henderson, R.A., Innes, B.M., Fergusson, C.L., Crawford, A.J., Withnall, I.W., 2011. Collisional accretion of a Late Ordovician oceanic island arc, northern Tasman Orogenic Zone. Australia. Australian Journal of Earth Sciences 58, 1-19.

Holcombe, R.J., Stephens, C.J., Fielding, C.R., Gust, D., Little, T.A., Sliwa, R., Kassan, J., McPhie, J., Ewart, A., 1997. Tectonic evolution of the northern New England Fold Belt: the Permian–Triassic Hunter–Bowen event. In: Ashley, P.M., Flood, P.G. (Eds.), Tectonics and metallogenesis of the New England Orogen. Geological Society of Australia Special Publication 19, pp. 52-65.

Jessell, M.W., Valenta, R.K., 1996. Structural geophysics: integrated structural and geophysical modelling. Computer Methods in the Geosciences 15, 303-324.

Johnson, E.L., Phillips, G., Allen, C.M., 2016. Ediacaran–Cambrian basin evolution in the Koonenberry Belt (eastern Australia): Implications for the geodynamics of the Delamerian Orogen. Gondwana Research 37, 266-284.

Kennett, B.L.N., Fichtner, A., Fishwick, S., Yoshizawa, K., 2013. Australian seismological reference model (AuSREM): Mantle component. Geophysical Journal International 192, 871-887.

Kennett, B.L.N., Fishwick, S., Reading, A.M., Rawlinson, N., 2004. Contrasts in mantle structure beneath Australia: relation to Tasman Lines? Australian Journal of Earth Sciences 51, 563-569.

Kley, J., Monaldi, C.R., Salfity, J.A., 1999. Along-strike segmentation of the Andean foreland: causes and consequences. Tectonophysics 301, 75-94.

Klootwijk, C., 2013. Middle–Late Paleozoic Australia–Asia convergence and tectonic extrusion of Australia. Gondwana Research 24, 5-54.

ACCEPTED MANUSCRIPT

Kositcin, N., Purdy, D.J., Brown, D.D., Bultitude, R.J., Carr, P.A., 2015. Summary of results — Joint GSQ–GA Geochronology Project: Thomson Orogen and Hodgkinson Province, 2012–2013. Queensland Geological Record 2015/02.

McLean, M.A., Betts, P.G., 2003. Geophysical constraints of shear zones and geometry of the Hiltaba Suite granites in the western Gawler Craton, Australia. Australian Journal of Earth Sciences 50, 525-541.

McLean, M.A., Rawling, T.J., Betts, P.G., Phillips, G., Wilson, C.J., 2008. Three-dimensional inversion modelling of a Neoproterozoic basin in the southern Prince Charles Mountains, East Antarctica. Tectonophysics 456, 180-193.

Miller, H.G., Singh, V., 1994. Potential field tilt—a new concept for location of potential field sources. Journal of Applied Geophysics 32, 213-217.

Miller, M.S., Becker, T.W., 2012. Mantle flow deflected by interactions between subducted slabs and cratonic keels. Nature Geoscience 5, 726-730.

Mills, K., David, V., 2004. The Koonenberry deep seismic reflection line and geological modelling of the Koonenberry Region, western New South Wales. Geological Survey of New South Wales Open, GS 2004/185.

Moresi, L., Betts, P.G., Miller, M.S., Cayley, R.A., 2014. Dynamics of continental accretion. Nature 508, 245-248.

Murray, C.G., 1994. Basement cores from the Tasman fold belt system beneath the Great Artesian Basin in Queensland. Department of Minerals and Energy, Queensland, Report Number - 0724252541.

Murray, C.G., Kirkegaard, A.G., 1978. The Thomson Orogen of the Tasman orogenic zone. Tectonophysics 48, 299-325.

Musgrave, R.J., 2015. Oroclines in the Tasmanides. Journal of Structural Geology 80, 72-98.

Neef, G., 2004. Stratigraphy, sedimentology, structure and tectonics of lower Ordovician and Devonian strata of South Mootwingee, Darling Basin, western New South Wales. Australian Journal of Earth Sciences 51, 15-29.

Nishiya, T., Watanabe, T., Yokoyama, K., Kuramoto, Y., 2003. New isotopic constraints on the age of the Halls Reward Metamorphics, North Queensland, Australia: Delamerian metamorphic ages and Grenville detrital zircons. Gondwana Research 6, 241-249.

Percival, I.G., 2010. Palaeontology Appendix. In: Greenfield, J., Gilmore, P., Mills, K. (Eds.), Explanatory notes for the Koonenberry Belt geological maps. Geological Survey of New South Wales, Bulletin 35, pp. 443–456.

PISA, 2006. Neoproterozoic – Ordovician Polygons. https://sarig.pir.sa.gov.au/Map.

Purdy, D.J., Carr, P.A., Brown, D.D., 2013. A review of the geology, mineralisation, and geothermal energy potential of the Thomson Orogen in Queensland. Geological Survey of Queensland, Record 2013/01.

Purdy, D.J., Cross, A.J., Brown, D.D., Carr, P.A., Armstrong, R.A., 2016. New constraints on the origin and evolution of the Thomson Orogen and links with central Australia from isotopic studies of detrital zircons. Gondwana Research 39, 41-56.

Radke, B.M., 2009. Hydrocarbon and Geothermal Prospectivity of Sedimentary Basins in Central Australia: Warburton, Cooper, Pedirka, Galilee, Simpson and Eromanga Basins. Geoscience Australia, Report Number - 192167203X.

Rawlinson, N., Kennett, B.L.N., 2008. Teleseismic tomography of the upper mantle beneath the southern Lachlan Orogen, Australia. Physics of the Earth and Planetary Interiors 167, 84-97.

Rawlinson, N., Kennett, B.L.N., Salmon, M., Glen, R.A., 2015. Origin of Lateral Heterogeneities in the Upper Mantle Beneath South-east Australia from Seismic Tomography. In: Khan, A., Deschamps, F. (Eds.), The Earth's Heterogeneous Mantle: A Geophysical, Geodynamical, and Geochemical Perspective. Springer, pp. 47-78.

ACCEPTED MANUSCRIPT

Rosenbaum, G., 2014. Geodynamics of oroclinal bending: Insights from the Mediterranean. Journal of Geodynamics 82, 5-15.

Rosenbaum, G., Gasparon, M., Lucente, F.P., Peccerillo, A., Miller, M.S., 2008. Kinematics of slab tear faults during subduction segmentation and implications for Italian magmatism. Tectonics 27, TC2008, doi:10.1029/2007TC002143.

Rosenbaum, G., Li, P., Rubatto, D., 2012. The contorted New England Orogen (eastern Australia): New evidence from U-Pb geochronology of early Permian granitoids. Tectonics 31, TC1006, doi: 0.1029/2011TC002960.

Spampinato, G.P., Betts, P.G., Ailleres, L., Armit, R.J., 2015a. Early tectonic evolution of the Thomson Orogen in Queensland inferred from constrained magnetic and gravity data. Tectonophysics 651-652, 99-120.

Spampinato, G.P.T., Ailleres, L., Betts, P.G., Armit, R.J., 2015b. Crustal architecture of the Thomson Orogen in Queensland inferred from potential field forward modelling. Australian Journal of Earth Sciences 62, 581-603.

Stevens, B.P.J., 1991. Northwestern New South Wales and its relationship to the Lachlan Fold Belt. Geological Society of Australia Abstracts, p. 50.

Stewart, J.R., Betts, P.G., 2010. Implications for Proterozoic plate margin evolution from geophysical analysis and crustal-scale modeling within the western Gawler Craton, Australia. Tectonophysics 483, 151-177.

Sun, X., Gravestock, D.I., 2001. Potential hydrocarbon reservoirs in upper levels of the eastern Warburton Basin, South Australia. Primary Industry and Resources South Australia, Report Book.

Swain, C.J., 2000. Reduction-to-the-pole of regional magnetic data with variable field direction, and its stabilisation at low inclinations. Exploration Geophysics 31, 78-83.

Thalhammer, O.A.R., Stevens, B.P.J., Gibson, J.H., Grum, W., 1998. Tibooburra Granodiorite, western New South Wales: emplacement history and geochemistry. Australian Journal of Earth Sciences 45, 775-787.

Veevers, J.J., 2000. Billion-year earth history of Australia and neighbours in Gondwanaland. Gemoc Press, North Ryde, New South Wales.

Veevers, J.J., 2004. Gondwanaland from 650–500 Ma assembly through 320 Ma merger in Pangea to 185–100 Ma breakup: supercontinental tectonics via stratigraphy and radiometric dating. Earth-Science Reviews 68, 1-132.

Verdel, C., Stockli, D., Purdy, D., 2016. Low-temperature thermochronology of the northern Thomson Orogen: Implications for exhumation of basement rocks in NE Australia. Tectonophysics 666, 1-11.

Webby, B.D., 1978. History of the Ordovician continental platform shelf margin of Australia. Journal of the Geological Society of Australia, 25, 41-63.

Whiting, T.H., 1986. Aeromagnetics as an aid to geological mapping—a case history from the Arunta Inlier, Northern Territory. Australian Journal of Earth Sciences 33, 271-286.

Withnall, I.W., Crouch, S.B.S., Woods, K.T., Henderson, R.A., Davis, B.K., 1995. Geology of the Southern Part of the Anakie Inlier, Central Queensland. Queensland Geology 7, p. 245.

Withnall, I.W., Golding, S.D., Rees, I.D., Dobos, S.K., 1996. K—Ar dating of the Anakie Metamorphic Group: Evidence for an extension of the Delamerian Orogeny into central Queensland. Australian Journal of Earth Sciences 43, 567-572.

Withnall, I.W., Henderson, R.A., 2012. Accretion on the long-lived continental margin of northeastern Australia. Episodes 35, 166-176.

Woodcock, N.H., Fischer, M., 1986. Strike-slip duplexes. Journal of Structural Geology 8, 725-735.

ACCEPTED MANUSCRIPT

Woodcock, N.H., Rickards, B., 2003. Transpressive duplex and flower structure: Dent fault system, NW England. Journal of Structural Geology 25, 1981-1992.

ACCEPTED MANUSCRIPT

ACCEPTED MANUSCRIPT

List of the Figures

Fig. 1 (a) Simplified geological map showing major tectonic elements in eastern Australia [abbreviations are: AI - Anakie Inlier, BP - Barnard Province, BGS - Bowen-Gunnedah-Sydney Basins, CB - Cooper Basin, CC - Curnamona Craton, CT - Charters Towers, GP - Greenvale Province, KB - Koonenberry Belt]. **(b)** Pseudocolour Bouguer gravity anomaly and **(c)** Pseudocolour RTP aeromagnetic images showing curvilinear ~E-W geophysical features at the southern Thomson Orogen. Black dots indicate borehole locations (1 - DIO Adria Down 1, 2 - GSQ Maneroo 1, 3 - AMX Toobrac 1, 4 - BEA Coreena 1, 5 - PPC Carlow 1, 6 - PPC Gumbardo 1, 7 - GSQ Mitchell 1, 8 - AOP Alba 1, 9 - Eromanga 1, 10 - Thargomindah 1, 11 - DIO Ella 1, 12 - Brewarrina 1) [abbreviations: LESZ - Louth-Eumarra Shear Zone; MA - Macquarie Arc; OF - Olepoloko Fault].

Fig. 2 (a) Bouguer gravity map (illuminated from northeast) showing major gravity trends (white dashed lines) in the southern Thomson Orogen and surrounding area [abbreviations are: BT – Bancannia Trough; CB – Cooper Basin; CC – Curnamona Province; CTO – Central Thomson Orogen; KZ – Kayrunnera Zone; LESZ – Louth-Eumarra Shear Zone; NLO – Northeast Lachlan Orogen; NR – Nebine Ridge; NT – Nelyambo Trough; STO – Southern Thomson Orogen; WZ – Wonnaminta Zone]. **(b)** Pseudocolour RTP aeromagnetic image of the study area (illuminated from northeast) showing major structural features [abbreviations are: BF – Boomi Fault; CF – Culgoa Fault; KF – Koonenberry Fault; KuF – Kulkyne Fractures; LF – Lawrence Fault; LMF – Little Mountain Fault; LESZ – Louth-Eumarra Shear Zone; MoF – Mount Oxley Fault; NF – Niccamucca Fault; OF – Olepoloko Fault; PF – Purnanga Fault; TF – Tongo Fault; ToF – Torowoto Fault; WiF – Willara Fault; F1, F2 and F3 – Unnamed faults]. **(c)** Solid geology map interpreted from geophysical datasets [modified after Hegarty (2010, 2011)].

Fig. 3 Simplified time-space diagram of the study area [sources: 1. Black (2006), 2. Black (2007), 3. Bodorkis et al. (2013), 4. Bultitude and Cross (2012), 5. Cross et al. (2015), 6. Draper (2006), 7. Fergusson et al. (2001), 8. Fergusson et al. (2007), 9. Fergusson *et al.* (2013), 10. Foden et al. (2006), 11. Fraser et al. (2014), 12. Glen et al. (1996), 13. Glen (2005), 14. Glen et al. (2010), 15. Glen et al. (2013), 16. Glen et al. (2014), 17. Greenfield et al. (2010), 18. Hegarty (2011), 19. Henderson (1983), 20. Henderson et al. (2011), 21. Kositcin et al. (2015), 22. Percival (2010), 23. PISA (2006), 24. Withnall and Henderson (2012), 25. Withnall et al. (1995), 26. Withnall et al. (1996)].

ACCEPTED MANUSCRIPT

Fig. 4 (a) 2D deep seismic reflection profile 99AGS C1, and **(b)** geological interpretation of the seismic profile showing the geometry of major faults in the Koonenberry Belt.

Fig. 5 (a, b) Colour shaded RTP aeromagnetic and Bouguer gravity images for the area shown in Figure 2a. White lines indicate State boundaries. **(c, d)** Tilt derivative image of (500m) upward continuation of RTP aeromagnetic data and composite image of RTP aeromagnetic data over the tilt derivative image with structural interpretation [abbreviations are: KF – Koonenberry Fault; OF – Olepoloko Fault; WiF – Willara Fault; F1, F2 and F3 – Unnamed Faults]. **(e)** Solid geology map of the area [abbreviations: CG – Currawinya Granite; GSG – Granite Springs Granite; HF – Hungerford Granite; EG – Ella Granite; TG – Tibooburra Granite; WG – Wolgolla Granite].

Fig. 6 (a, b) Pseudocolour RTP aeromagnetic and tilt derivative of (500m) upward continuation of RTP aeromagnetic images for the area shown in Figure 2b. **(c, d)** Composite images of RTP aeromagnetic data over the tilt derivative image with structural interpretation and solid geology map of the area. [abbreviations are: KF – Koonenberry Fault; KUF – Kulkyne Fractures; LMF – Little Mountain Fault; MoF – Mount Oxley Fault; OF – Olepoloko Fault; PF – Purnanga Fault; TF – Tongo Fault; ToF – Torowoto Fault; WiF – Willara Fault; BG – Barrona Granite; HF – Hungerford Granite; TD - Tinchelooka Diorite].

Fig. 7 (a - f) Tilt derivative image of RTP aeromagnetic data and structural interpretation for the areas shown in Figure 6. [abbreviations are: KUF – Kulkyne Fractures; LMF – Little Mountain Fault; MoF – Mount Oxley Fault; OF – Olepoloko Fault; PF – Purnanga Fault; TF – Tongo Fault; ToF – Torowoto Fault; WiF – Willara Fault].

Fig. 8 (a) Combined image of 2D deep seismic reflection profiles 05GATL 1 and 05GATL 2. **(b)** Geological interpretation of the seismic profile showing the geometry of the Olepoloko Fault and the crustal architecture at the Thomson-Lachlan boundary.

Fig. 9 (a-d) Tilt derivative image of RTP aeromagnetic data and structural interpretation for the area shown in Figure 5. F1, F2 and F3 are unnamed faults.

Fig. 10 (a, b) Pseudocolour RTP aeromagnetic and tilt derivative of (500m) upward continuation of RTP aeromagnetic images for the area shown in Figure 2b. **(c, d)** Composite images of RTP aeromagnetic data over the tilt derivative image with structural interpretation and solid geology map of the area. [abbreviations are: BT –Brevelon Tank area, KW – Kenilworth; BF – Boomi Fault; CF – Culgoa Fault; NF – Niccamucca Fault; KT – Keats

ACCEPTED MANUSCRIPT

Thrust Fault; MoF – Mount Oxley Fault; LESZ – Louth-Eumarra Shear Zone; LMF – Little Mountain Fault; RF – Rookery Fault; WTF – White Tank Fault; MFT – Mulga Tank Fault; F4, F5, F6 and F7 – Unnamed faults; TPC – Tarcoon Pluton Complex; ByG – Byrock Granite].

Fig. 11 (a) Shallow seismic reflection profile (DMR 98-02) across the Culgoa Fault. **(b)** Geological cross-section constructed from the seismic profile.

Fig. 12 Schematic structural evolution models of the southern Thomson Orogen showing the possible development and activation of the faults from **(a)** Delamerian, **(b)** Benambran and **(c)** Tabberabberan orogenies. [The light green coloured area represents the southern Thomson Orogen; abbreviations are: CF – Culgoa Fault; KF – Koonenberry Fault; KuF – Kulkyne Fractures; LF – Lawrence Fault; LMF – Little Mountain Fault; LESZ – Louth-Eumarra Shear Zone; MoF – Mount Oxley Fault; NF –Niccamucca Fault; OF – Olepoloko Fault; PF – Purnanga Fault; TF – Tongo Fault; ToF – Torowoto Fault; WiF – Willara Fault; F1, F2 and F3 – Unnamed faults].

Fig. 13 Horizontal slice through the AuSREM mantle model [modified after Kennett et al. (2013)] for P-wave speed at 100 km depth.

Fig. 14 Greyscale aeromagnetic image (50% transparent) shows the possible evolution of eastern Australia as revealed by present-day location of different subduction systems (colour coded with time) [modified after Glen (2005); Glen (2013); Glen et al. (2013)].

ACCEPTED MANUSCRIPT

ACCEPTED MANUSCRIPT

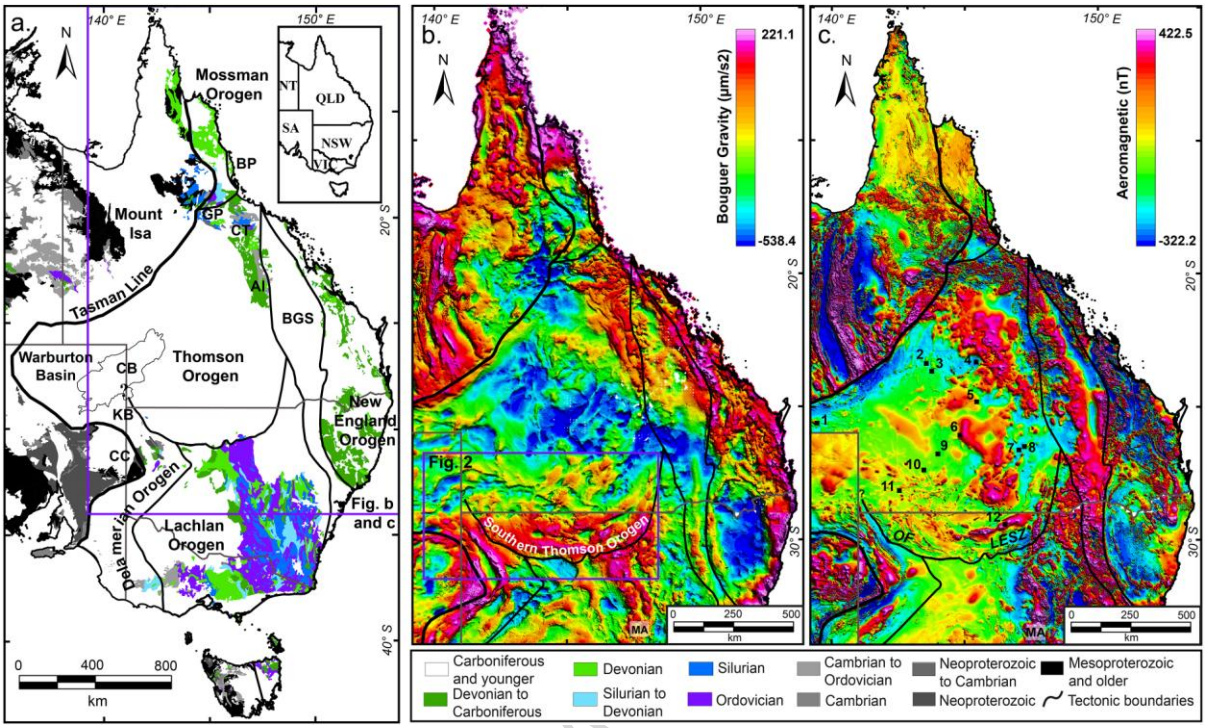

Fig. 1

ACCEPTED MANUSCRIPT

ACCEPTED MANUSCRIPT

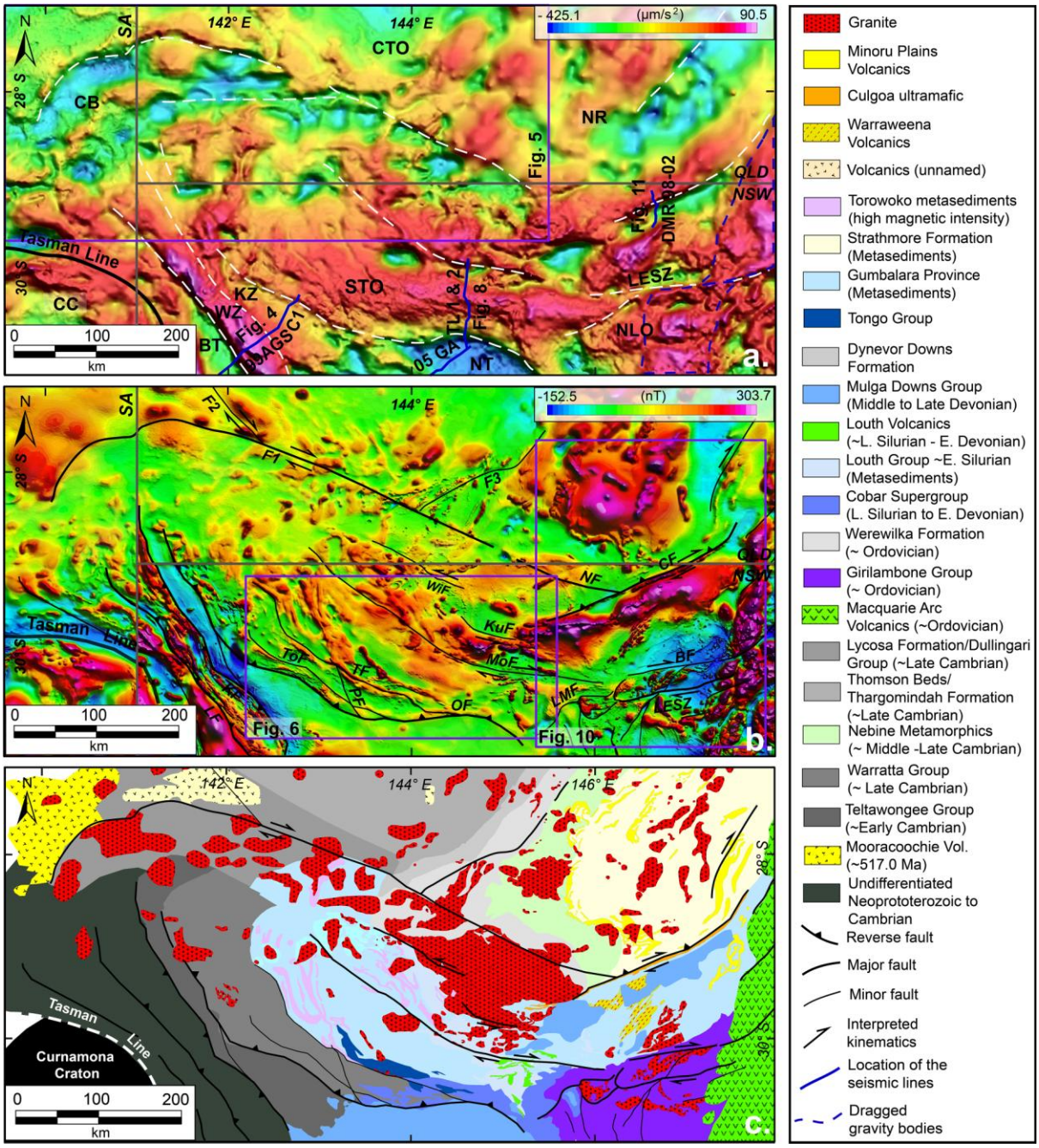

Fig. 2

ACCEPTED MANUSCRIPT

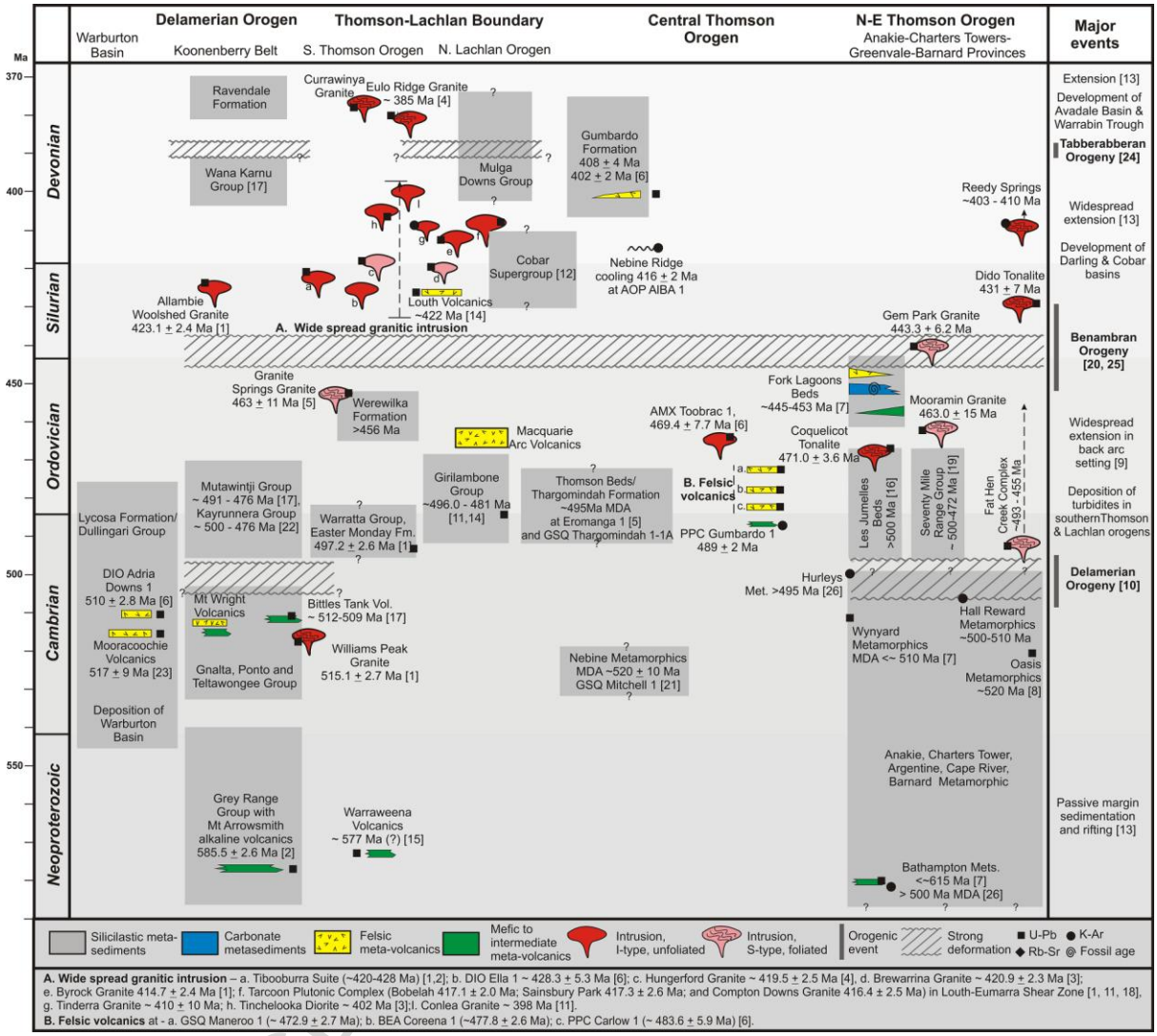

Fig. 3

ACCEPTED MANUSCRIPT

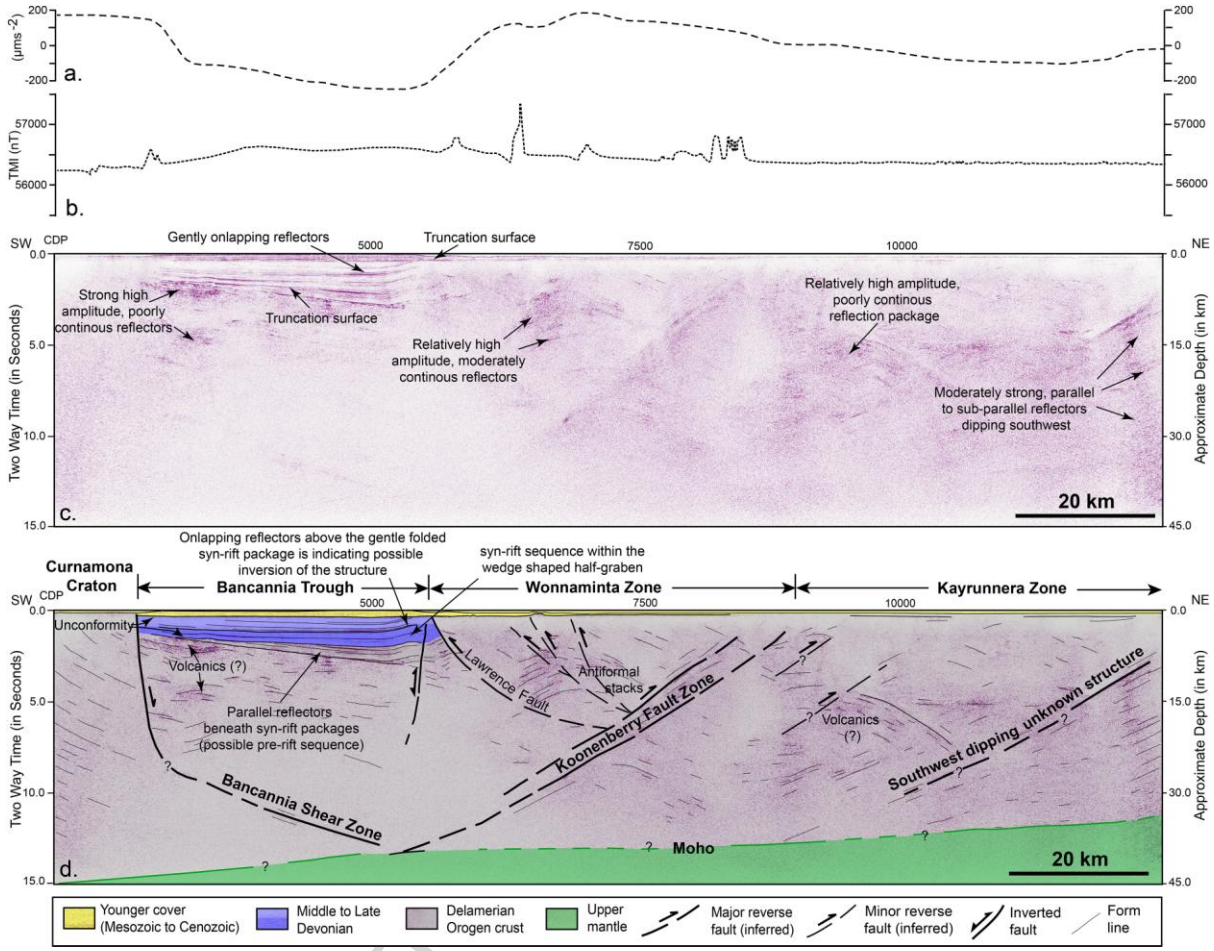

Fig. 4

ACCEPTED MANUSCRIPT

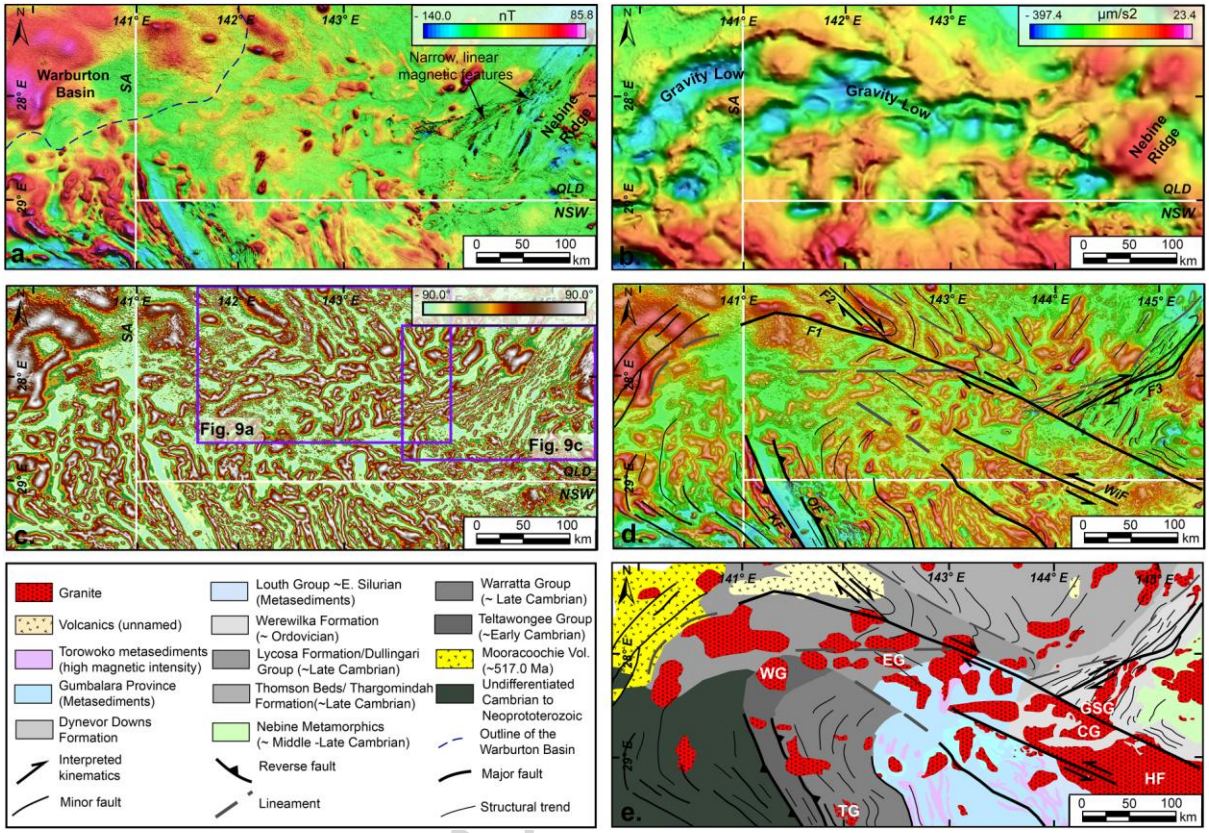

Fig. 5

ACCEPTED

ACCEPTED MANUSCRIPT

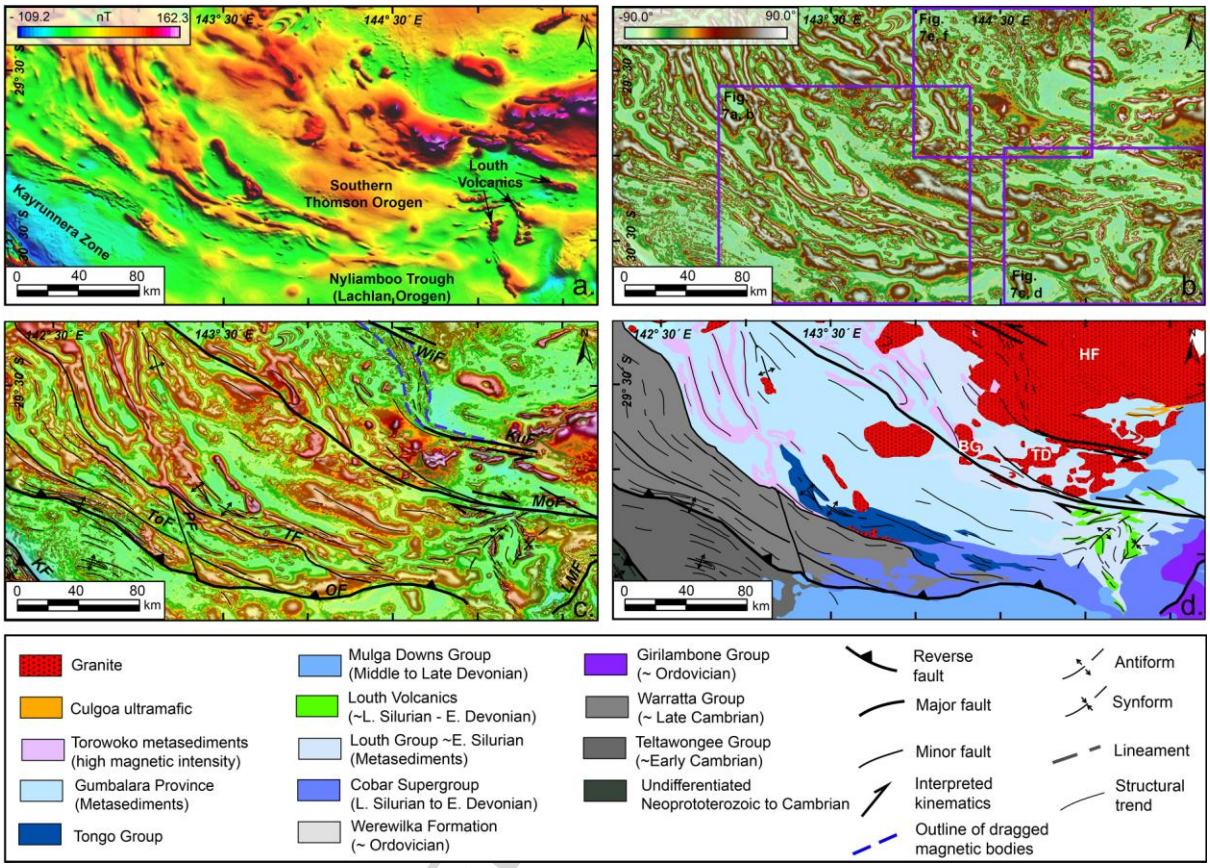

Fig. 6

ACCEPTED

ACCEPTED MANUSCRIPT

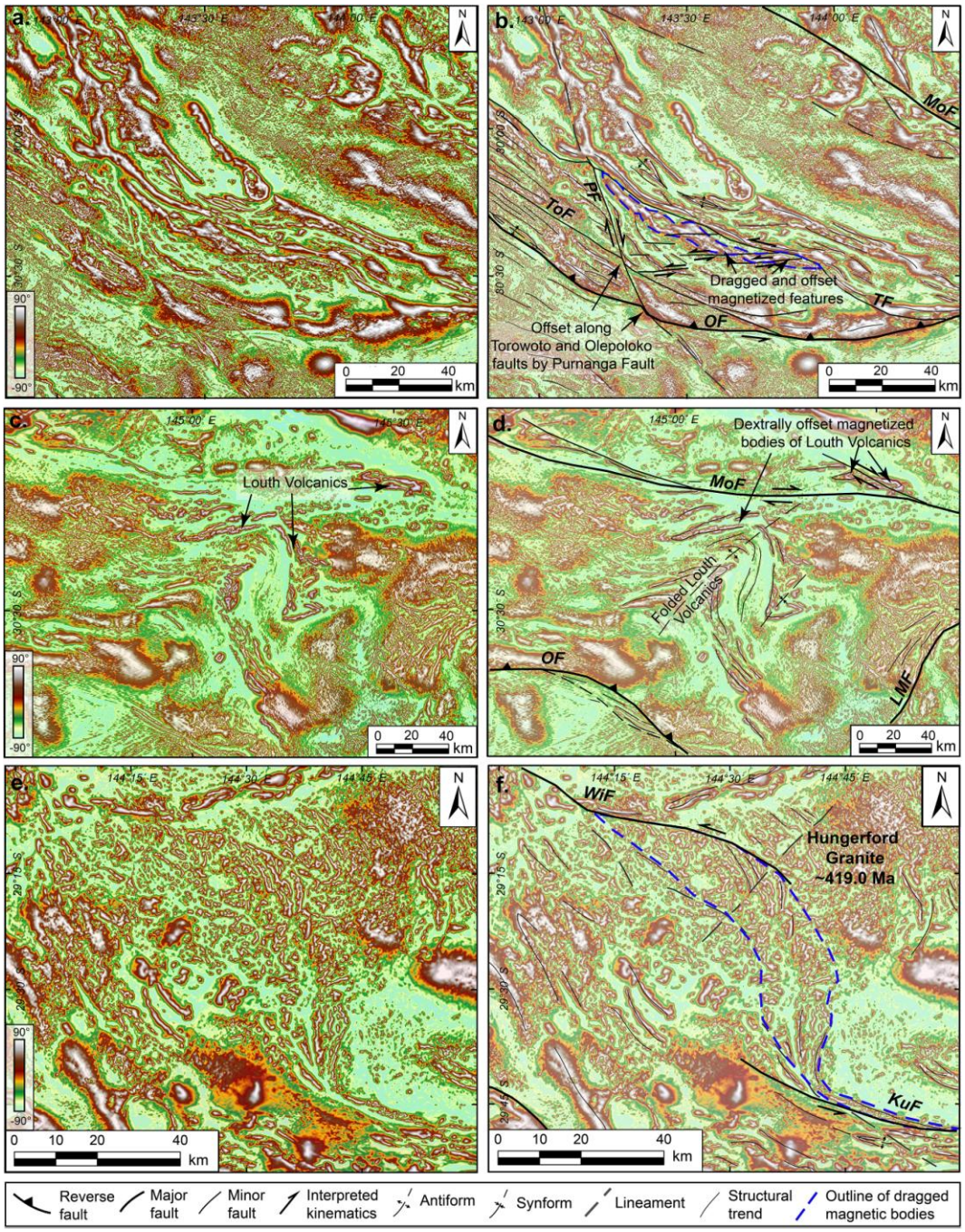

Fig. 7

ACCEPTED MANUSCRIPT

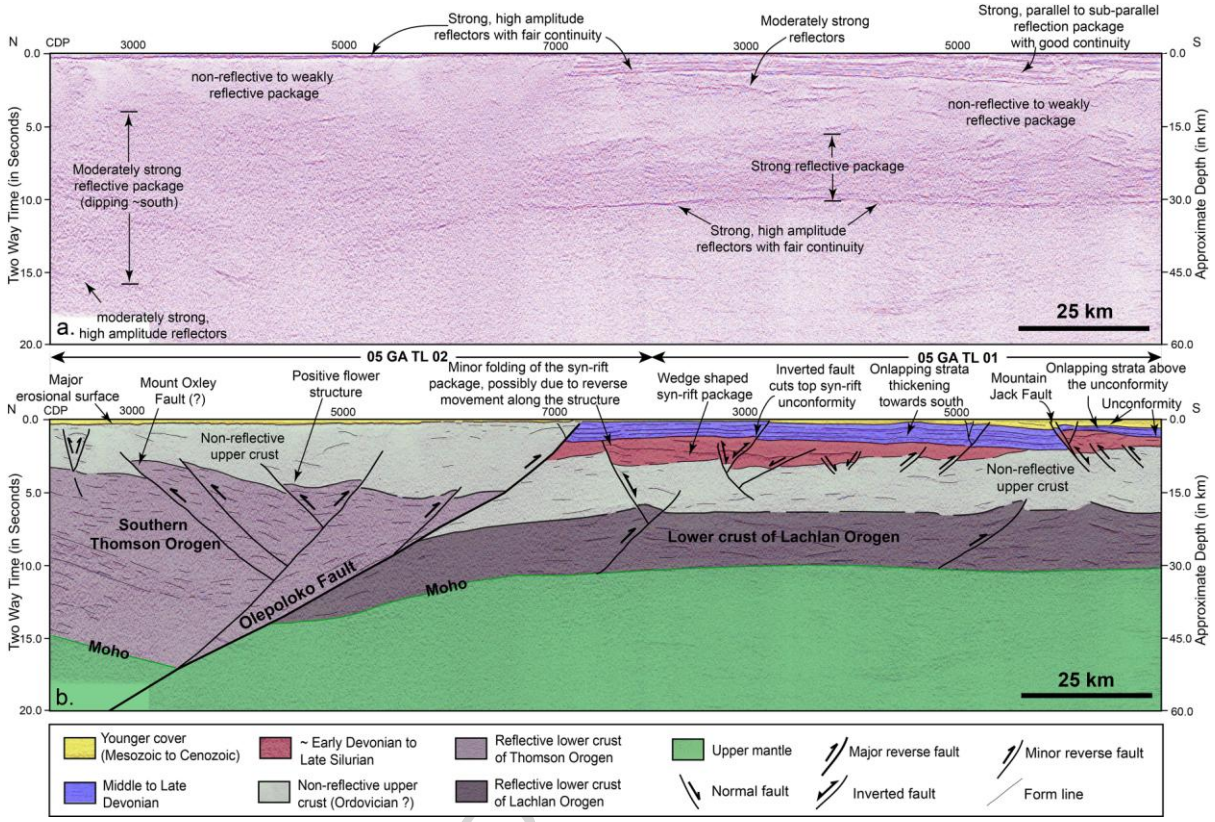

Fig. 8

ACCEPTED

ACCEPTED MANUSCRIPT

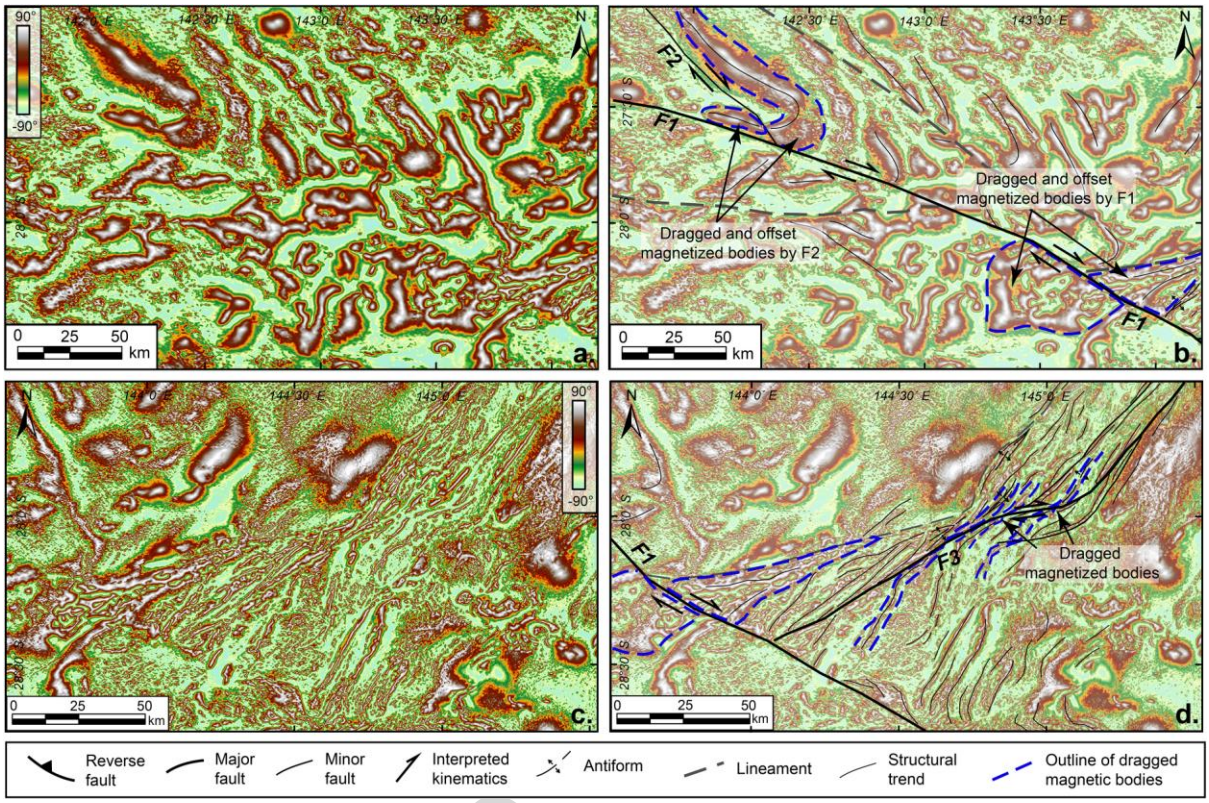

Fig. 9

ACCEPTED

ACCEPTED MANUSCRIPT

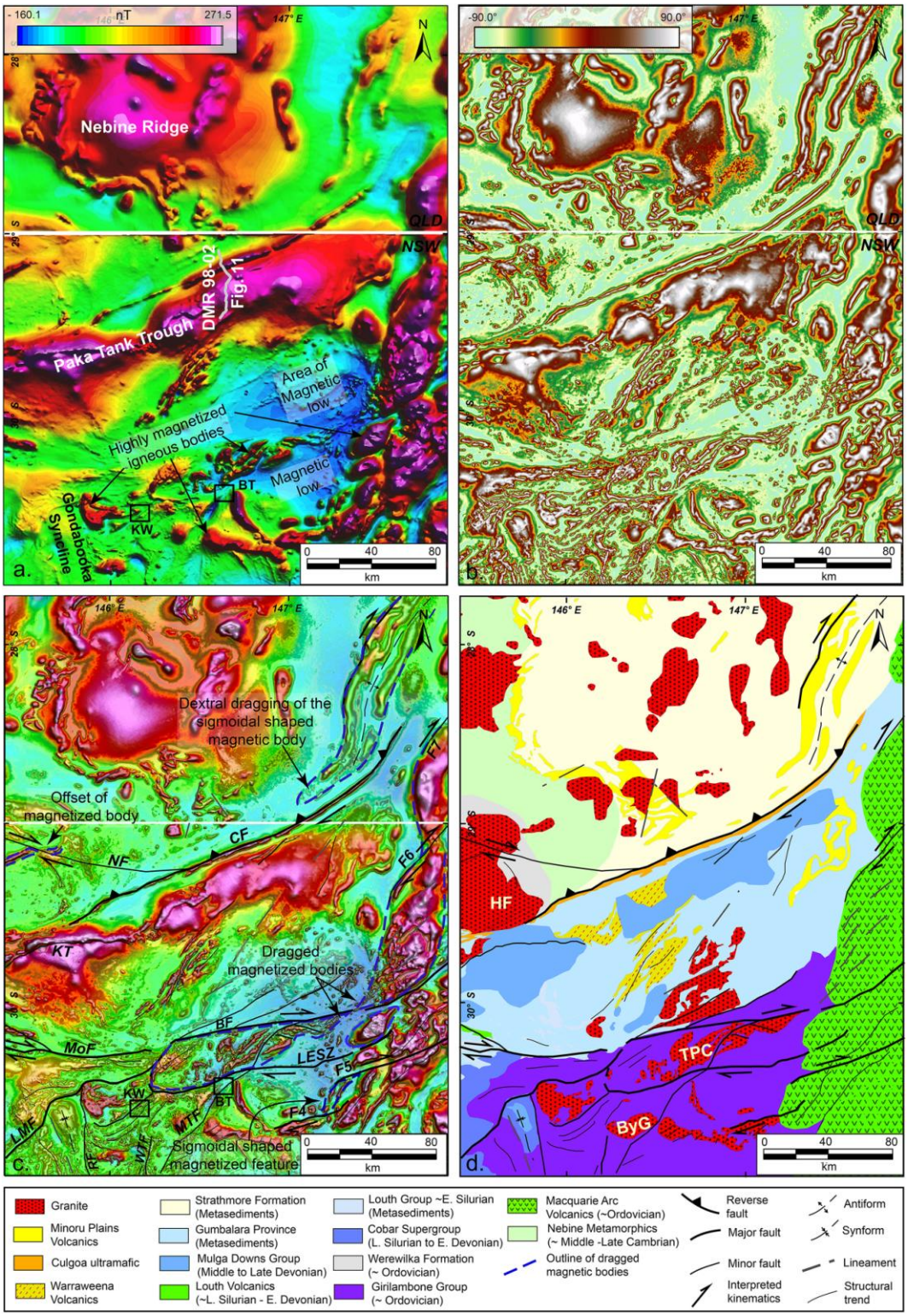

Fig. 10

ACCEPTED MANUSCRIPT

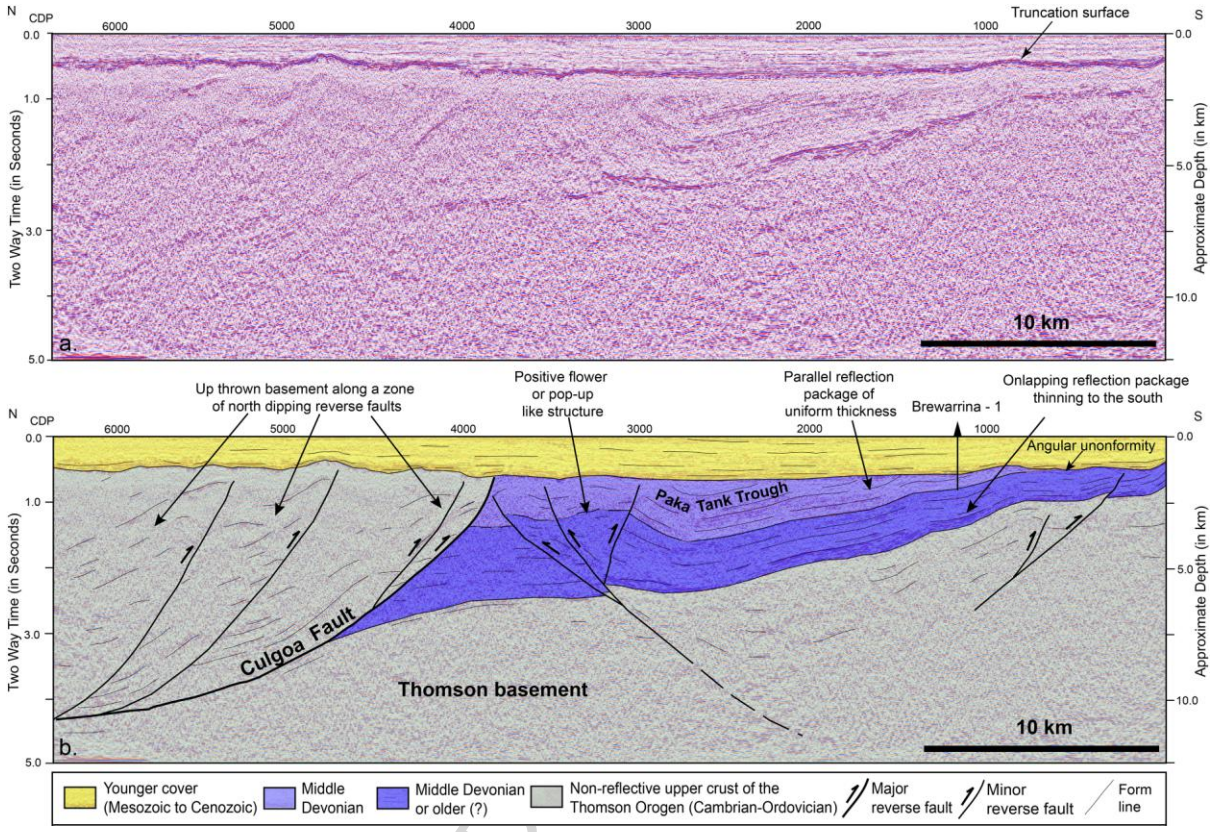

Fig. 11

ACCEPTED

ACCEPTED MANUSCRIPT

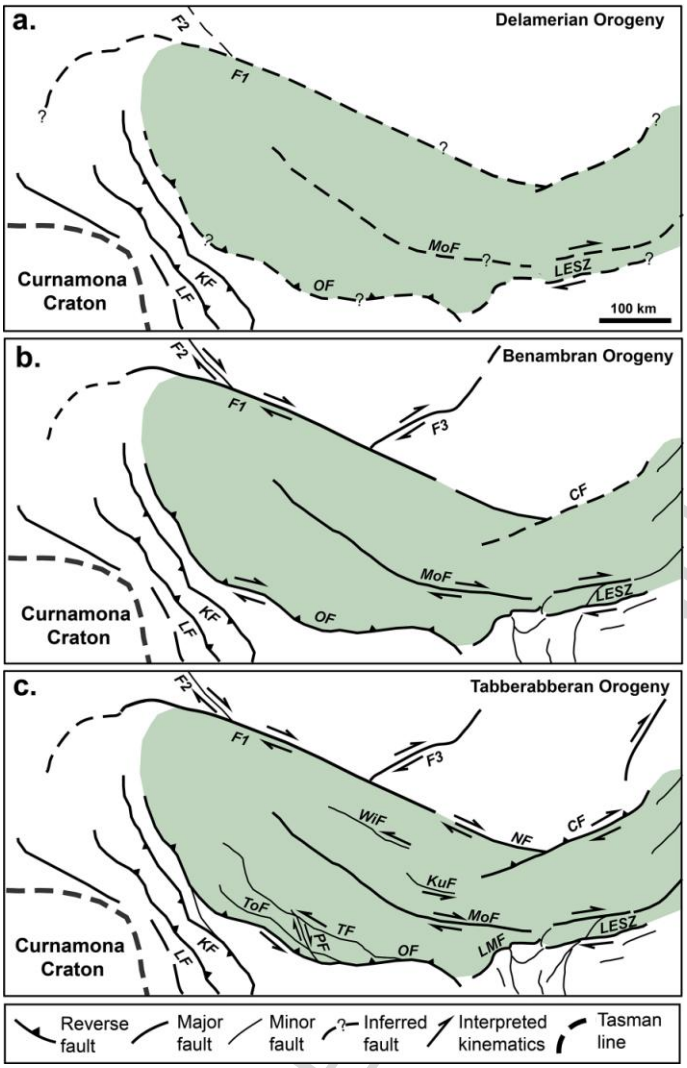

Fig. 12

ACCEPTED MANUSCRIPT

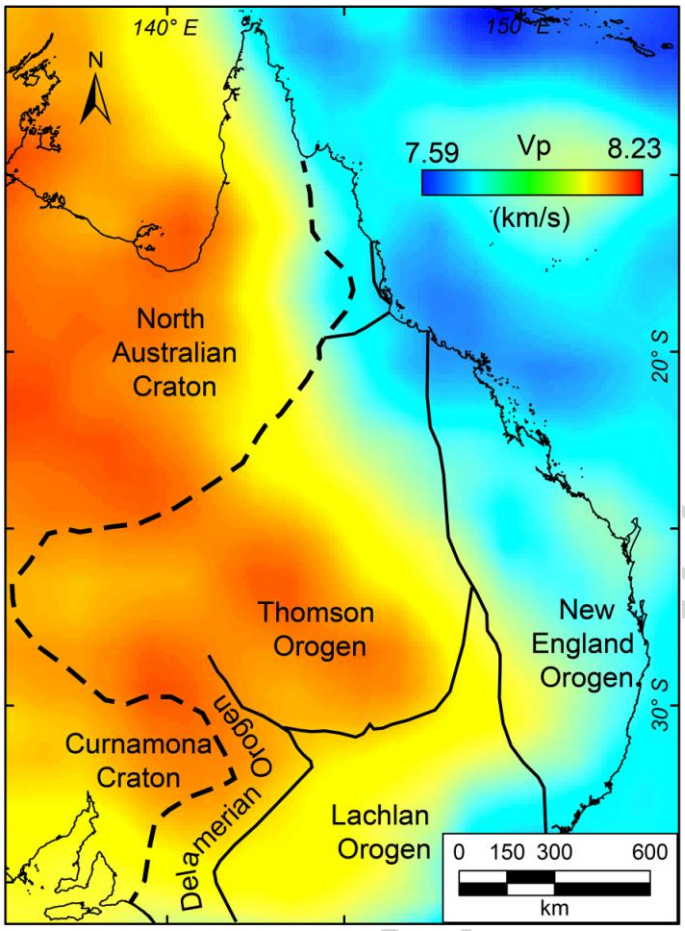

Fig. 13

ACCEPTED MANUSCRIPT

ACCEPTED MANUSCRIPT

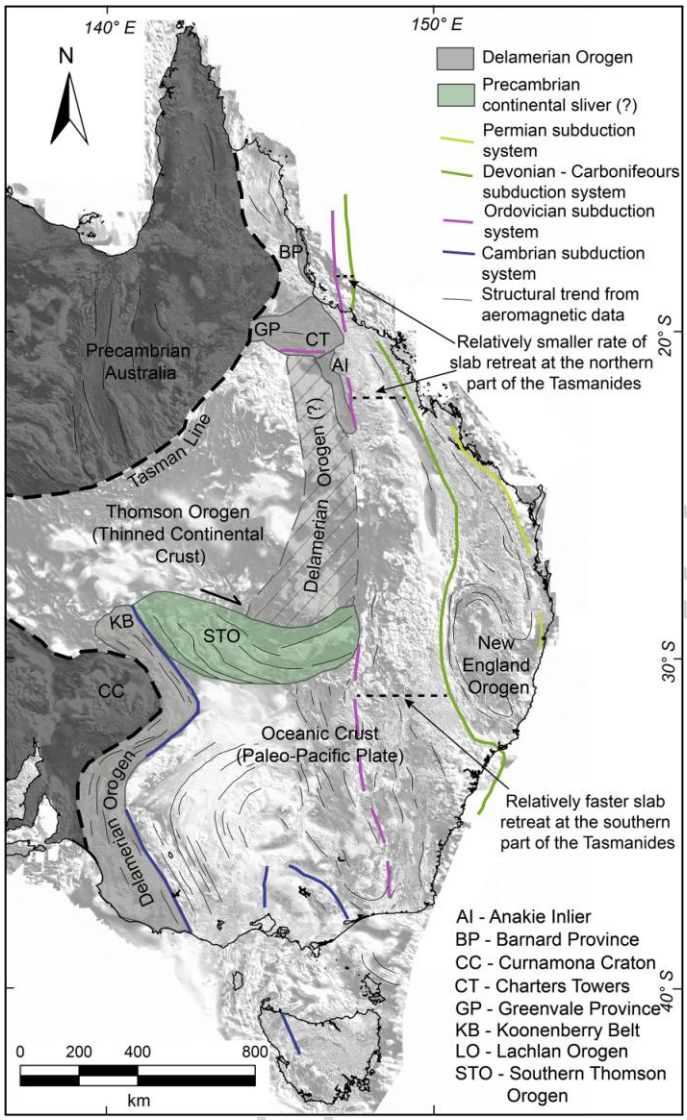

Fig. 14

ACCEPTED MANUSCRIPT

Highlights:

- Crustal-scale orogen-perpendicular structures occur in the central Tasmanides.
- Structures accommodated multiple episodes of Paleozoic deformation.
- Fault kinematic indicators show dextral, sinistral and reverse motions.
- Crustal and lithospheric thickness variations occur across the structures.
- The structures were possibly associated with lithospheric segmentation.

ACCEPTED MANUSCRIPT